ADHESION OF SMALL METAL SPHERES TO PLANE METAL SUBSTRATES

Thesis for the Degree of Ph. D.
MICHIGAN STATE UNIVERSITY
DOUGLAS FRANCIS ST. JOHN
1969



This is to certify that the thesis entitled

Adhesion of Samll Metal Spheres to

Plane Metal Substrates

presented by

Douglas Francis St. John

has been accepted towards fulfillment of the requirements for

Ph. D. degree in Mechanics

Major professor

Date May 8, 1969

ADHESION OF SMALL METAL SPHERES TO PLANE METAL SUBSTRATES

Ву

Douglas Francis St. John

AN ABSTRACT OF A THESIS

Submitted to
Michigan State University
in partial fulfillment of the requirements
for the degree of

DOCTOR OF PHILOSOPHY

Department of Metallurgy, Mechanics, and Materials Science

1969

ABSTRACT

ADHESION OF SMALL METAL SPHERES TO PLANE METAL SUBSTRATES

By

Douglas Francis St. John

In the conventional treatment of adhesion between a small solid object and a plane substrate, the object is considered to be a particle, and the adhesive force is taken to be the normal force necessary to remove it from the substrate. When this force is determined by the usual centrifuge method wherein the separating force acts perpendicular to the surface, it is found to be much greater than when determined by an electrostatic method or indeed, by mechanical methods other than perpendicular centrifugation. Our experiments, conducted with gold and silver spheres of 10μ to 60μ -diameter removed by various methods from gold, silver, and nickel plane substrates of various roughnesses, suggest that the spheres cannot be treated as particles, but rather must be regarded elastic or plastic bodies of noninfinitesimal extent as whose adhesion is controlled by the tangential component of the applied force. Presumably this tangential force produces an initial rolling to break the adhesion at the points of contact.

Centrifuge runs at varying zenith angle (that is, the angle between the direction of the applied force and the normal to the plane) indicate that particle adhesion is a function of zenith angle and the hardness of the adherents, particularly of the substrate. For relatively soft substrates, the minimum adhesion force occurs at zenith angles greater than 90°. In these cases, it is shown that plastic deformation or crushing of the asperities or points of contact has caused the center of rotation of the sphere to shift and thereby to reduce the resultant adhesion couple arm. The experimental results from the zenith angle centrifuge runs are interpreted on the basis of a plastic-deformation model.

ADHESION OF SMALL METAL SPHERES TO PLANE METAL SUBSTRATES

Ву

Douglas Francis St. John

A THESIS

Submitted to
Michigan State University
in partial fulfillment of the requirements
for the degree of

DOCTOR OF PHILOSOPHY

Department of Metallurgy, Mechanics, and Materials Science

1969

ACKNOWLEDGMENTS

My endeavor was made pleasurable by Professor D. J.

Montgomery's constant encouragement and counsel, so necessary
in the work leading to an experimental thesis. His varied
and profound background, and cheerful attitude was also a
valuable aid.

Almost all of the Owens-Illinois Okemos Research Laboratory staff made contributions to the work in this thesis.

In particular, thanks are due to Dr. M. S. Hall and Mr. E.

A. Oster for their discerning and sympathetic attitude,

Messrs. F. H. Brown, J. D. Grier, R. N. Clark, Dr. L. J.

Taylor and Dr. R. F. Schaufele for their helpful suggestions,

and Mr. R. H. Moore for his skillful design and fabrication

of equipment.

My thanks also go to Professors T. Triffet for thesis guidance and serving as Guidance Committee Chairman; L. E. Malvern, for helpful discussions on analyses of results; and to F. J. Blatt and R. H. Wasserman who also served on my guidance committee.

The vacuum deposited gold and chromium substrates were skillfully prepared by Mr. B. R. Emch, Owens-Illinois, Inc., Toledo, Ohio.

I would also like to express thanks to Mrs. L. Howe for typing several rough drafts of the thesis.

The research has been supported by Owens-Illinois, Inc. through a cooperative part-time employment graduate-fellow-ship arrangement. I am very grateful to Mr. F. H. Buell, Dr. J. W. Hackett, and Dr. J. M. Teague for making this arrangement possible.

Most importantly, my wife, Beverly, has been a constant source of encouragement during the course of the work.



TABLE OF CONTENTS

CHAPTE	₹	Page
ı.	INTRODUCTION	1
II.	BASIC CONSIDERATIONS	4
	Technological and Scientific Importance	4
	Theoretical Considerations	5
	Background	9
	Laws	9
	Previous Experiments	10
	Methods	11
	Choice of Method and System	15
	Proposed Mechanism	16
III.	EXPERIMENTAL PROCEDURE AND RESULTS	19
	Significant Variables	19
	Methods	20
	Centrifuge	21
	Precision of the Ultracentrifuge Method	22
	Particle or Object Deposition	23
	Microphotographic Evaluation	24
	Cassette	24
	Trials	26
	Electrostatic	28
	Force Calculations	28

TABLE OF CONTENTS (Continued)

CHAPTER				Page
Trials		•	•	30
Inconsistency of Results	•	•	•	31
Combined Techniques	•	•	•	33
Surface Roughness	•	•	•	35
Two Dimensional Model		•	•	35
Electrostatic Tangential Experiments		•		41
Centrifuge Zenith Angle Evaluations .	•	•	•	42
Apparatus		•	•	42
Adherents		•	•	44
Experimental Results	•	•	•	44
Discussion of Experimental Results			•	48
Interpretation of Results	•		•	51
REFERENCES	•	•	•	68
λ DDENDT V				73

LIST OF FIGURES

FIGUR	E	age
1.	Microphotograph of gold spheres on single-crystal germanium substrate	25
2.	Centrifugal removal force vs sphere radius .	27
3.	Schematic diagram of cell for electrostatic method	29
4.	Electrostatic removal force <u>vs</u> sphere radius for silver spheres	32
5.	Schematic diagram for combined centrifugal and electrostatic method	34
6.	Removal force vs sphere radius, combined method	36
7.	Sphere resting in a vee-slot	37
8.	Calculated reaction forces F_1 relative to applied force \underline{vs} wedge angle	39
9.	Reaction forces F_2 relative to applied force \underline{vs} wedge angle	40
10.	Schematic of cassette for zenith angle centri- fugal runs	43
11.	Centrifugal removal force vs zenith angle for various radii gold spheres	45
12.	Centrifugal removal force \underline{vs} sphere radius at various zenith angles	46
13.	Centrifugal removal force vs zenith angle for various radii gold spheres	47
14.	Centrifugal removal force vs sphere radius at various zenith angles	49
15.	Model for sphere on plane	52



IHE

LIST OF FIGURES (Continued)

Page	IGURE
54	16. Normalized sliding and pulling removal force vs zenith angle
56	17. Normalized rolling removal force vs zenith angle
60	18. Uniform stress distribution resulting from applied force
62	19. Normalized removal force <u>vs</u> zenith angle for shift of center-of-rotation
63	20. Uniform stress distribution resulting from applied force and 0.375b shift in center of rotation
76	Measured force <u>vs</u> calculated force for disc and hemisphere
78	A2. Measured force vs calculated force for sphere-

I. INTRODUCTION

The art of making adhesive bonds is older than science, and a large number of disconnected ideas, rules, and traditions have been accumulated. The term solid-to-solid adhesion has come to mean different things to different people. Solid-to-solid adhesion may be defined as the state in which the surfaces of two solids are held together by interfacial forces. Solid-to-solid adhesion does not require the presence of a bonding substance between two materials, but only the presence of two materials sufficiently close to each other to have interactions occur.

Both experimental and theoretical attacks of the problem are complicated. In 1929, P. A. M. Dirac wrote:

... the underlying physical laws necessary for the mathematical theory for a large part of physics and the whole of chemistry are thus completely known, and the difficulty is only that the exact application of these laws lead to equations much too complicated to be soluble.³

In the case of solid-to-solid adhesion and particularly adhesion of small particulate matter $(10^{-1}\mu$ to $10^3\mu$ in diameter), the fundamental laws describing the microscopic interactions are known, but no general procedure is available to interpret these microscopic interactions at a macroscopic level. For the most part, the difficulty in

developing a theory of the force acting across an interface is inventing a mathematically tractable model that is any reasonable approximation to physical reality.4

Our understanding of the interactions occurring at and near the interfaces of two solids in "contact" is far from satisfactory. For even the simplest of geometries and materials, there has been neither theoretical treatment of any rigor nor experimental study of any completeness. Even with the most ambitious theoretical models available, investigators in this field have been forced to make drastic simplifying assumptions. The most serious problem is that very few laws have been established through which a theory could be developed. In an attempt to remedy this situation, we undertook a program of experimental and theoretical investigation simple enough that it might contribute to advancing the understanding of the solid-to-solid interactions across interfaces. We chose materials as well defined as practicable, namely gold and silver spheres on gold, silver and nickel substrates. As our major parameter we chose a mechanical variable, the direction of applied force, a variable that other investigations have not paid much attention to. We investigated other variables including material properties and ambient conditions, such as size of particulate matter, cover gas, temperature, pressure and substrate hardness. Most of the experimental work was completed by the centrifuge method, after an insight to the mechanism of particle removal had been acquired by use of an electrostatic technique.

The formal statement of the problem is the following:

For a sphere adhering to a macroscopically smooth plane substrate, to predict as a function of radius of sphere and properties of materials, the force acting through the center of gravity of the sphere, necessary to remove the sphere at a given zenith angle.

II. BASIC CONSIDERATIONS

Technological and Scientific Importance

A better understanding of the fundamentals of adhesion of particulate matter to solid substrates would advance the technology of several industries. In some cases, one wants particles to stick to substrates, for example, in crop dusting, filtering and separating of solids, contamination, and air pollution control, and xerography. In other cases, one wants particles not to adhere to substrates, for example, in removal of solid soil in cleaning and washing, filtering and separating of solids, pelletizing and briquetting, and pneumatic conveying of bulk material. Specific illustrations under current investigation are the recontamination of the Voyager Lander and Viking systems with microbes, and the reduction of hazards from radioactive debris and other metal and ceramic powders.

In principle, one needs only to sum the gradients of potentials integrated over a six dimensional space in order to calculate an adhesive strength between two solid materials. For several reasons, even crude computations of the force of adhesion (or cohesion) are not feasible: First, the intermolecular potential functions are not well enough

known. Next, the microscopic structure of even a crystalline surface is not sufficiently well understood in detail;
the structure of an amorphous surface is even less understood. For noncrystalline systems, moreover, certain data
necessary for these computations may never be obtainable,
for example, the radial-pair-distribution functions for noncrystalline materials composed of complex molecules cannot
be determined because intramolecular x-ray scattering prevents the determination of intermolecular distances.7

Theoretical Considerations

Several authors have tried to correlate interatomic and molecular forces with adhesive forces as measured by various techniques. To simplify the correlation, some force contributions are neglected: moreover, at least one adjustable parameter is inserted to obtain the correct order of magnitude of force values. This adjustable parameter usually relates to the gap between particulate matter and substrates, or to some assumption concerning the interface.8

The possible forces that could act across the interface between a particle and a substrate may be put into perspective by a consideration of the fundamental particle interactions. These interactions fall into four categories: Strong (nuclear), Moderately Strong (electromagnetic), Weak (decay), and Very Weak (gravitational). For particles in the size range from 10μ to 60μ -diameter, the adhesive force swamps the graviational interactions. Moreover, distances

are so large that nuclear forces, either weak or strong, play no role in solid-to-solid adhesion. Hence, the only interactions of interest are those of electrical origin as manifested in quantum mechanics. Classification of these electromagnetic forces is somewhat arbitrary, since they may be grouped as to their chemical nature or their physical nature. History and tradition, moreover, have also played havoc with classification of these forces. When microscopic forces are evidenced in a macroscopic assembly, they are manifested in different forms which historically and traditionally have led to such names as surface tension, capillary forces, 10 hydrogen bonding, weak-electron-sharing bonding, 11 Stephen viscosity effect, and mechanical hooking. 12

The forces arising from particle interactions which are electrical in nature may be more or less logically divided into three types - short range-forces, intermediate-range forces, and long-range forces. The short-range forces which may be called chemical forces, arise when molecules come close enough together for their electron probability-distribution clouds to overlap. On the other hand, long-range forces are those which arise when the electron probability-distribution clouds do not overlap. Finally, the intermediate-range forces sometimes known as second-order exchange forces, are important at intermediate distances. An example is the interatomic potential associated with helium.

The potentials arising from long-range forces vary as the inverse powers of the intermolecular separation. These potentials may be conveniently divided into three parts:

(1) the electrostatic contribution, (2) the induction contribution, and (3) the dispersion contribution. The electrostatic and induction contributions may both be explained by application of straightforward electrostatic considerations from Maxwell's equations, whereas the dispersion forces need to be explained by quantum mechanics. 14

Potential energy arising from <u>electrostatic contributions</u> between particles emanates from interactions of "multipole moments". These multipole moments may be charges (monopoles), dipole moments, quadripole moments, etc. The application of Coulomb's Law of electrostatic attraction yields the potential functions for various types of interactions between two molecules, most conveniently handled by expansion of charge distribution in multipoles. For an assembly of a large number of molecules, of course, the statistical average of the potential function must be used, as Keesom, for example, has done in the calculation of dipoledipole interactions. 15

Induction effects result from a multipole's inducing multipoles in a neighboring molecule by polarization. The interaction of a permanent multipole with a neighboring multipole induced by induced by it is called the induction effect. Debye¹⁶ calculated the dipole-molecule force for a permanent dipole moment's inducing a dipole in a neighboring molecule by polarization.

The interaction of multipoles induced within neighboring charge distributions is called the dispersion effect. London dispersion forces appear in the second-order perturbation terms in a quantum mechanical calculation of the energy of interaction between two molecules. 17,18,19 This effect. a general interaction occurring between any two molecules or atoms which are in close proximity, is independent of their permanent dipoles. Even though the time-averaged multipoles are zero, instantaneous deviations from spherical symmetry will produce multipoles capable of yielding dispersion effects. For spherical molecules the dispersion potential function for the induced-dipole-induced-dipole varies as the inverse 6th power of the separation distance. Further terms in the dispersion energy vary as r⁻⁸ (induced-dipole - induced-quadripole), r⁻¹⁰ (induced-quadripole induced-quadripole), and so on. For large distances (200 angstroms) the London dispersion forces must be modified because of the diminishing effect resulting from electromagnetic retardation. 20,21 For the induced-dipole - induceddipole case, the interaction potential energy now varies inversely as the 7th power of the distance instead of the 6th power.

The effect of van der Waals' attraction for the molecular potential energy between two spheres has been computed by de Boer²² and by Haymaker.²³ Experiments on the van der Waals' attraction between two plates have been performed by Deryagin,²⁴ Overbeek²⁵ and Sparnaay.²⁶ By weighing

techniques, they measured forces of the order of a few micrograms. The force variation was found to be roughly proportional to $1/h^4$. Kitchener and Prosser²⁷ have obtained results like those of Sparnaay.

Except for special cases, 28,29,30 it is not possible to conduct experiments to measure the forces at distances smaller than 10⁻⁵ cm, because the surfaces are not truly flat. Correlations of measured forces with those predicted theoretically have in the past only been accomplished by assuming a distance of closest approach. In general, the measured bond strength is equal to the maximum possible bond strength reduced by the following factors: loss of strength due to separation of molecules, loss of strength due to internal stresses, and changes in internal stresses due to testing forces.³¹

Background

A monumental effort has been put into the study of adhesion and adhesive performance. An article on adhesion may cite over a hundred references in support of a particular view of the theory of adhesion. These theories fall into one or more of the following categories: surface energy, molecular forces, electrostatic forces, and mechanical forces.

<u>Laws</u>

Several laws concerning sliding friction, rolling friction, and solid-to-solid adhesion have been proposed since

Amontons' paper on Friction in 1699.³² In general, the laws of rolling and sliding friction assume that the resistance to rolling is almost entirely due to losses in the deformed solid and that the adhesion component is not large compared to the joining force.³³ In general, the rules and laws of adhesion and friction apply to two objects whose dimensions are large compared with the surface roughness of either object.

Previous Experiments

Adhesion of solid particles to solid substrates has been discussed from a general point of view by Corn, 34 Morgan, 35 and Fuchs. 36 Most references, however, tend to emphasize one or the other theories of adhesion, implying, and sometimes stating, that others are not important. Bickerman suggests that solid-to-solid adhesion is due to viscosity, capillary pressure, and electrostatic attraction. 37 Bowden and Tabor postulated that if two solids are placed in contact with combined normal and tangential forces, "welding" occurs at the interface. 38 In 1966, Krupp and Sperling proposed a theory of adhesion between small solid particles and a solid wall. Their theory is based on van der Waals' forces of attraction between the adherents, to cause irreversible deformation at their interface. 39 The theory takes into account electrostatic forces but neglects capillary effects. Krupp and his co-workers, by the ultracentrifuge method, measured the adhesive strength of gold

particles on quartz, gold, polyester, polyamide, and regenerated cellulose in nitrogen and in air at various relative humidities. What ler et al., by an ultracentrifuge method, measured the force of adhesion of polymer particles (5μ to 30μ -diameter) adhering to a selenium surface as a function of the triboelectric charge generated on the surfaces of the particles prior to adhesive contact, and as a function of surface charge on the selenium. Fish 42 , 43 has estimated the electrostatic forces of adhesion between particles, and the electrostatic force on a conductive sphere sitting on a charged conductive plane.

Methods

Properties of adherents, geometrical configuration, magnitude of adhesive forces, and so on, must be considered in the choice of a method to measure adhesive forces. The forces controlling separation depend upon the manner which separation occurs, e.g., pulled off, slid off, or rolled off. The bulk of experiments in the past are based on a picture in which particles are separated by normal forces; removal is then characterized by a single variable. On the other hand, if the separating force is not normal, the removal can be characterized by a couple with or without sliding, which implies a frictional force. In practice, the particle may be removed by any of these effects under different conditions.

The traditional methods used to measure adhesion of particles to substrates or to other particles, generally fall into the following categories: (1) weighing method, (2) pendulum method, (3) vibration and impulse techniques, (4) aerodynamical method, (5) friction method, (6) disc method, and (7) centrifuge method. Besides these traditional methods, an electrostatic method can be employed.

The weighing method was used by Tomlinson, 44 Bradley, 45,46 Eauser, 47 and Abenroth.48 The adhesive force is simply measured by either a spring or gravitational balance. The method suffers primarily from the fact that only a single datum concerning the adhesive force between the adherents can be obtained on a given run. With very small particles (10 μ to 60 μ -diameter), moreover, a difficulty arises in attaching the particles either to a fixed support or to the weighing instrument.

In the <u>pendulum method</u> (inverted inclined plane) gravity is the driving force which removes particles or objects from substrates. Here, the removal force -- mass m times gravitational acceleration g -- is composed of two components, one normal to the substrate and the other tangential to the substrate. Both the normal and tangential components of the total mg force are determined by the zenith angle at which the pendulum is placed. This method has been successfully used by McFarlane⁴⁹ and Howe, ⁵⁰ but only for particles whose density and size are large enough that the mg forces exceed the adhesive forces. This condition does not hold for very

small particles. Inherent in the pendulum method is the fact that the force for <u>normal</u> removal must be larger than the force for tangential removal.

Vibration techniques and impulse techniques have been used to measure the adhesive forces between large samples of particles and substrates. The technique can be used in a high vacuum but suffers from the fact that both the forces generated and the accelerations imparted cannot be defined explicitly, although this difficulty is currently being attacked effectively.⁵¹

Several investigators, namely Jordan, ⁵² Gillespie, ⁵³

Masironi, ⁵⁴ Larson, ⁵⁵ and Bagnold, ⁵⁶ have used the <u>aerodynami-cal method</u> to determine adhesion between dust or particles to solid substrates. As with vibration and impulse techniques, the ill-defined aerodynamic conditions of the method leads to difficulty in interpreting the results.

Amontons' Law is the basis for the <u>friction technique</u> to measure adhesive forces, particularly between particles and substrates. This method is similar to the pendulum method, with one primary difference. Here, the zenith angle (<u>i.e.</u>, the angle between the direction of the applied mg force and the outward normal from the substrate) varies from π to $\pi/2$ radians, whereas in the pendulum method the zenith angle varies from $\pi/2$ to 0 radians. Bowden and Tabor⁵⁷ and Deryagin⁵⁸ have shown that Amontons' Law must be either restricted or modified to describe adequately the forces applied to particles on substrates. Several investigators

which include Cremer, ⁵⁹ Patat and Schmid, ⁶⁰ and more recently Berg et al., ⁶¹ have used the friction method or modifications thereof to determine adhesive forces between particles and substrates. As in the pendulum method, particles must be heavy enough to be removable by their weight. The interdependencies between adhesion and friction (either sliding or rolling) complicate the analysis.

The surface forces associated with colloidal suspensions and dispersions have been investigated by Marshal et al., 62 and Hull et al., 63 by the rotating disc technique. The technique appears to be applicable only for immersed systems such as collodial suspensions, and is included here only for completeness.

Centrifuge techniques to measure particle adhesion have been used by Beams^{64,65} in 1930, by Gillespie⁶⁶ in 1955, by Bohme et al., since 1956,⁶⁷ and more recently by Kordecki and Orr⁶⁸ in 1960, Enlow,⁶⁹ in 1968, and Donald,⁷⁰ in 1969. The process consists of dusting particles on a substrate, inserting it into a cassette placed in a rotor-tube bore and accelerated in discrete steps to various levels. The substrate and particles are microphotographed before and after each discrete run. The method has the advantage that many particles may be simultaneously investigated. The force is usually applied normal to the substrate, but some investigators have positioned the substrate in such fashion that the force is tangential.

An <u>electrostatic method</u>, which apparently has not been reported in the literature, can be a useful technique for measuring adhesion when both the particles and the substrate are sufficiently conductive to allow charging of the particles in an electric field. A plane substrate electrode supporting the particles together with a second electrode, may be housed in a vacuum or pressure chamber to avoid dielectric breakdown of the gas. Alternatively, a gas with a higher breakdown strength, such as a Freon, may be utilized. Care must be taken to avoid particle-particle or particle-substrate electrostatic interactions which provide an undeterminate tangential component to the applied forces.

Choice of Method and System

To simplify the system, well-defined materials were selected. Initially, gold atomized spheres and plane gold substrates were chosen, because this element is little affected by ambient conditions such as temperature, pressure, and composition of the atmosphere. Because the materials are identical and conductive, effects of contact potential and triboelectrification are eliminated. Both the centrifuge method and the electrostatic method were employed.

Runs with the centrifuge are tedious because of the start-stop technique required with the available apparatus. Results did show a first power dependence on sphere radius, as reported in 1930 by Bradley. Initial calculations for the electrostatic method suggested that the forces due to

electric field strength obtainable in air at standard conditions were not sufficient to remove the particles. The experiment was tried despite the negative predictions. The particles came off with less than the force required in the centrifuge technique. The observed force for removal was nearly independent of particle size, particles of any radius coming off at approximately the same potential at a given gap. The inconsistency between the electrostatic experiments and the centrifugal runs forced us to investigate the mechanism of separation, and in particular to study the combined effects. We conjectured that tangential forces (in the electrostatic experiment) as well as normal forces might be set up by inhomogenieties in the substrate or by fields from other particles.

In practice, particles are seldom removed by forces applied normally. Hence, we decided to examine the variation of the removal force with direction on which the force is applied, and how this variation is affected by the geometrical parameters of particle radius and roughness of substrate surface, and the mechanical and electrochemical properties of the material.

Proposed Mechanism

We conjectured that in the combined runs the adhesive normal force plus the tangential component due to the electrical inhomogenieties initially caused particles to roll and thereby break the adhesive bond. This conjecture implies

that the adhesive force and couple were higher statically (while stuck) than dynamically (while rolling). The model suggested varying the zenith angle. The centrifuge cassette was modified so that the zenith angle could be varied in order to study the couple and force relationships. For example, if the zenith angle is set at 90°, the adhesion is due to an adhesive couple alone, since the applied force is purely tangential; if the zenith angle is 0° , the adhesion is due to an adhesive force alone, since the applied force is purely normal, as in traditional centrifuge methods. We hoped to predict the dependence of the force on angle from only two runs, at zenith angle equal to 90° and to 0° . Generally, the force of removal for the gold spheres on gold substrates at 90° was approximately 5% to 10% of that at 0° . But on going past a zenith angle of 900, for gold on gold, the inertial force necessary for particle removal decreased: This finding implied that the proposed mechanism was inadequate to explain experimental results of this type; it might well apply, however, to combinations of other materials. We concluded that in such cases plastic deformation must constitute the controlling factor, in accordance with a model to be described later. This conclusion suggested studying mechanical parameters such as hardness of the material. An estimate of the local stresses by Hertz's formulas for elastic deformation showed this conjecture based on plastic deformation to be reasonable. To confirm this hypothesis, experiments were made with other materials. Indeed, when the

compressive stresses in the substrate appear to be above the elastic limit, the mechanism can be described by a plastic model.

III. EXPERIMENTAL PROCEDURE AND RESULTS

Significant Variables

From a practical standpoint, the phenomena of interest in solid-to-solid adhesion are the forces of adhesion as they are evidenced in the mechanism of removal of particles from substrates. These phenomena are simply manifestations of the short-range, intermediate-range, and long-range intermolecular forces in conjunction with continuum mechanics for real material objects. The dependent variable of primary interest in this treatment will be the force necessary to remove objects from a substrate. This force to be specified in both magnitude and direction will be a function of several independent variables.

We shall group the independent variables into sets pertaining to the materials, to the ambient conditions, and to the mechanical variables characterizing the adhesion phenomena. The variables are: 72

- I. Material Properties
 - A. Chemical Composition
 - 1. Body of Adherents
 - 2. Surface of Adherents
 - B. Molecular Structure
 - C. State of Strain of Adherents

- D. Yield Strength
- E. Compressive and Tensile Strength
- F. State of Electrical Charge
- G. Hardness of Adherents

II. Ambient Conditions

- A. Temperature
- B. Pressure
- C. Composition
- D. Electromagnetic Fields

III. Mechanical Variables

- A. Method of Contact
- B. Size of Particulate Matter
- C. Shape of Particulate Matter
- D. Surface Finish of Adherents
- E. Direction of Applied Force.

In addition to the above variables, there are others of importance such as contacting pressure between the adherents, area of contact, resitivity of the adherents, and time of contact, but are considered to be implied or determined by specifications of the above variables.

Methods

The aerodynamical method and the friction method provide information on adhesion, but they bury the information in the experimental data. For smaller particles, that is, in the size range of 1μ to $10\mu\text{-diameter},$ the weighing, pendulum, and friction methods are unsuitable. Vibration

and impulse techniques do not yield data which are easily reducible to quantitative interpretation.

As stated earlier, the experiments chosen for spheres of 10μ to 60μ -diameter on solid substrates are based on the centrifuge method and the electrostatic method. Both allow determination of object-substrate adhesive forces for many particles in one experiment.

Centrifuge

The centrifuge technique is the following: The substrate is placed in a cassette fitting into one of the tube bore holes of the rotor of the centrifuge, the adherent (object) having been previously attached to the outer wall of the substrate by one of several techniques. The rotor is accelerated stepwise to a speed at which the object is detached. The adhesive force is calculated from:

 $F_{adhesion} = m\omega^2 R$,

where m = mass of object

 ω = angular velocity

R = rotor arm distance between center of gravity
 of object and centrifuge axis.

As employed here, the centrifuge technique is an inherently tedious method since discrete start-stop runs must
be made to determine detachment forces. As a rule, speed
was increased in steps of the square root of two so that
the limiting applied force increased by a factor of two.

After each discrete centrifuge run, the substrate was microphotographed to determine object removal.

In all centrifuge experiments the apparatus was a Beckman Model L2-65B preparative ultracentrifuge with either a Type-60 Ti or Type-21 rotor. The ultracentrifuge is designed with solid-state electronic components for completely automatic control of speed and temperature. Actual rotor speed can be maintained within \pm 1% of the settings at speeds from 170 to 1,100 rps, and within 2 rps at speeds from 10 to 170 rps. For slower runs the speed was monitored within ± 1% by a General Radio Company Strobotac Type 1531-AB. The Type-21 rotor is provided with ten 3.81 cm-diameter tube bores in which the cassettes holding the object-covered substrates are inserted. Maximum speed for this rotor is 350 rps, with maximum centrifugal forces 59,164 g. In contrast to the Type-21 rotor, the Type-60 Ti fixed-angle rotor can attain a maximum speed of 1,000 rps, with maximum centrifugal forces of 361,300 g. This rotor is provided with eight 2.54 cm-diameter tube bores. With either rotor the centrifuge may be operated at either a pressure of 10^{-3} mm Hg or atmospheric pressure within the rotor tube bore. Acceleration and deceleration times are dependent upon the speed required, and are less than 10^3 seconds.

<u>Precision of the Ultracentrifuge Method</u> - The precision (or, otherwise stated noise level) of the ultracentrifuge method of measuring adhesion is estimated in the following

manner: Random shocks due to handling and microscopic evaluations are assumed to be less than 10 g, that is, the force (whether tensile or shear) will be less than 9,806 m dynes, where m is the mass of the particle in grams. Thus, particles with an adhesive force less than 9,806 times the mass may possibly be jarred loose from the substrate; this value will be considered the noise level or precision to which the adhesive forces can be determined. For spherical particles:

$$p = m_{\alpha} = 4\pi a^{3} \alpha \rho/3$$
where ρ = particle density (g/cm³)
$$\alpha = 10g$$

$$g = 980.6 \text{ cm/sec}^{2}$$

$$a = \text{particle radius (cm), or}$$

$$P = 4.11 \times 10^{4} \text{ a}^{3} \rho \text{ (dynes)}$$

For a 20µ-diameter gold sphere,

$$\rho = 19.31 \text{ g/cm}^3, \text{ and}$$

$$P = 4.11 \times 10^4 \ (10^{-3})^3 \ (19.31)$$

$$P = 0.793 \times 10^{-3} \text{ dyne} \ .$$

But, for a 2μ -diameter silver sphere, the noise level equals 0.431×10^{-6} dyne. Thus, the noise level or precision of a force measurement is dependent upon both the density and size of particles in question.

<u>Particle or Object Deposition</u> - To place particles on the plane substrate, we have tried several methods, including liquid sedimentation, camel's hair brush, air

settling, and fluidized bed. The most uniform dusting with fewest agglomerates, that is particles touching particles, was achieved by carefully vibrating or shaking a camel's hair brush previously dipped into the particle container. Particles from a broad size distribution (2μ to 60μ -diameter) can be dusted on one substrate efficiently. The dusting techniques are evaluated by viewing through a microscope. A properly dusted substrate is one in which few particles contact one another as seen in Figure 1.

Microphotographic Evaluation - A properly dusted area of the substrate is microphotographed before the initial run. For particles in the 10μ to $60\mu\text{-range}$, we used an overall magnification of approximately 80x--130x, including photographic magnification. For particles in the 2μ to $10\mu\text{-}$ range, the overall magnification ranged from 130x to approximately 450x. After each discrete run in the centrifuge, the same area was located on the substrate and re-photographed. A before-and-after particle comparison was made to determine which particles became detached in the previous centrifuge run. The substrate and particles are accelerated in the centrifuge at stepwise increased speeds until all particles of interest are detached from the substrate.

<u>Cassette</u> - The dusted substrate is housed in a cassette fitting into the tube bore of the rotor. For centrifuge runs for normally applied forces the cassette is placed into the tube bore of the centrifuge rotor in such a manner that

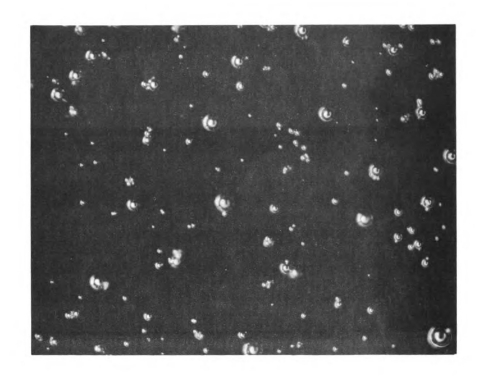


Figure 1.--Microphotograph of gold spheres on singlecrystal germanium substrate, magnification 135%.

the applied force necessary to overcome the centrifugal acceleration is normal to the surface of the substrate. Microphotographs of the dusted substrate can be obtained through a window in the cassette initially, and after each incremental centrifugation.

Trials - Adhesion of gold and silver spheres (Metz Refining Co., South Plainfield, N.J.) to a polycrystalline gold substrate (Alpha Metals, Inc., Jersey City, N.J. -1.27 cm-diameter by 0.013 cm-thick disc, Lot No. B9995) at 60% R.H., S.T.P. and at a pressure of 10^{-3} mm Hg was measured as a function of particle radius by means of the ultracentrifuge with the Type-21 rotor. The adhesion forces were determined by microphotographic evaluation of the particles remaining on substrates after each run. For gold and silver spheres in the 10μ to 60μ -diameter range, the force of adhesion, as measured by the centrifuge, varies approximately as the first power of the radius. For gold spheres the weight of the particle equals the adhesion force for about a 250μ particle, whereas for silver spheres the forces are equal for a 325μ to 400μ particle. Figure 2 shows a logarithmic plot of adhesion force vs particle size.

Centrifuge runs at a pressure of 10^{-3} mm Hg at 18° C, with the Ti-60 rotor carrying single-crystal silver cylinders, both (100) and (111) orientations, on which spherical silver particles have been dusted show an adhesion force that is independent of crystal orientation. Results indicate that the adhesion force is approximately proportional to the first

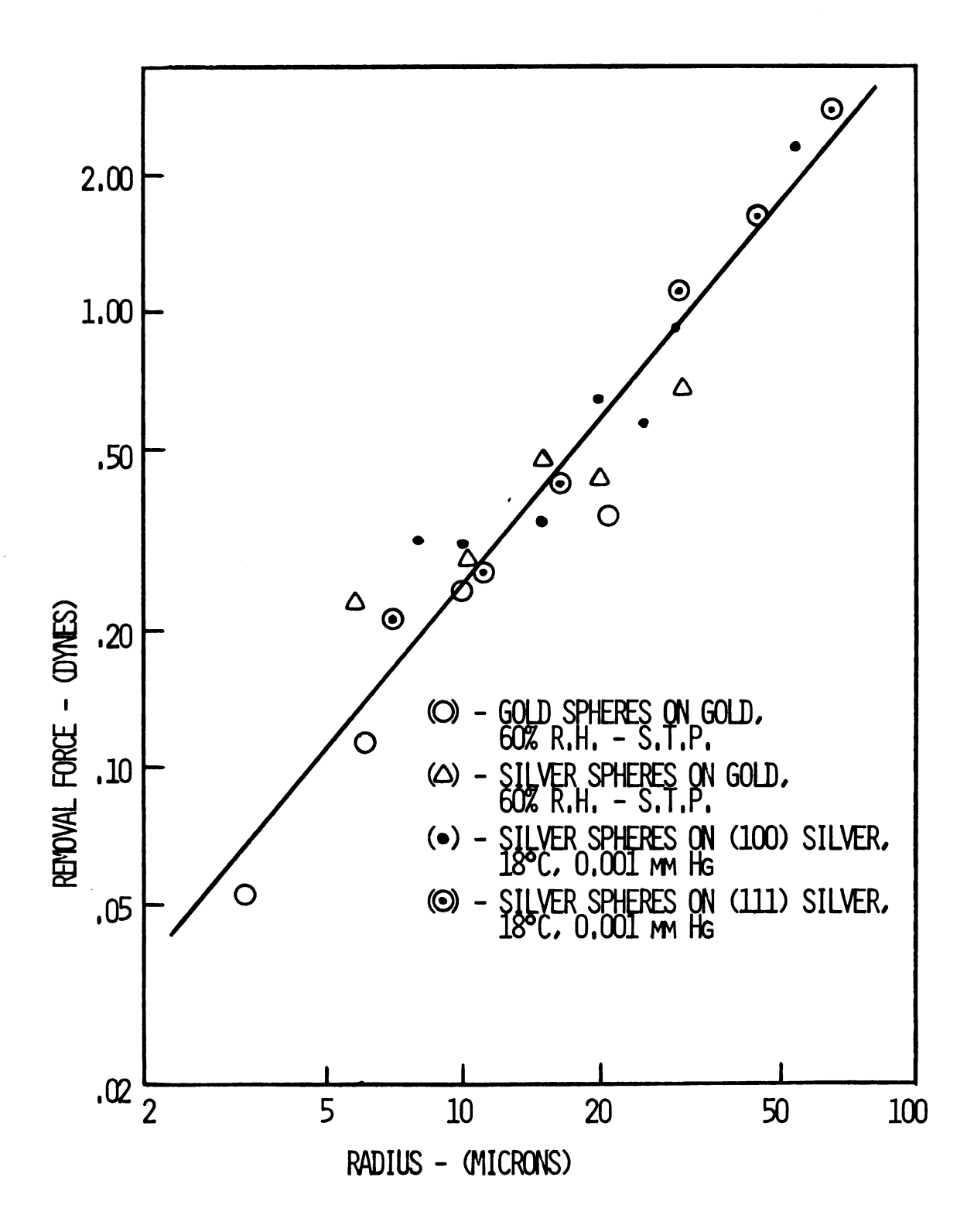


Figure 2. Centrifugal removal force vs sphere radius.

power of the radius for the silver spheres, as seen in Figure 2.

Electrostatic

An electrostatic method was devised for measuring adhesion of conductive particles to conductive substrates.

Cells were fabricated which are essentially parallel-plate capacitors, the bottom electrode being the substrate, the upper electrode consisting of a NESA (stannic oxide conductive coating) glass to allow microscopic observations during application of electric fields. A schematic of the cell can be seen in Figure 3. This method lends itself to continuous variations as opposed to the discrete or stepwise operations in the centrifuge.

The precision or noise level, the means of dusting the particles onto the substrates, and the microphotographic evaluation are the same in the electrostatic method as in the centrifuge method.

Force Calculations - The forces acting on a conductive Sphere resting on a conductive substrate in a uniform DC electric field are estimated from the following formulas:

$$F = \pi^5 \in _0 E_0^2 a^2 / 18 \text{ (mks)}^{73}$$

and
$$F = 1.537 \times 10^{-10} R^2 E_0^2 (mks)^{74}$$

where $\pi^5 \in_0 / 18 \approx 1.505 \times 10^{-10}$ and a = R.

These formulas were verified by experiment; for further details, see the Appendix. These formulas apply only when

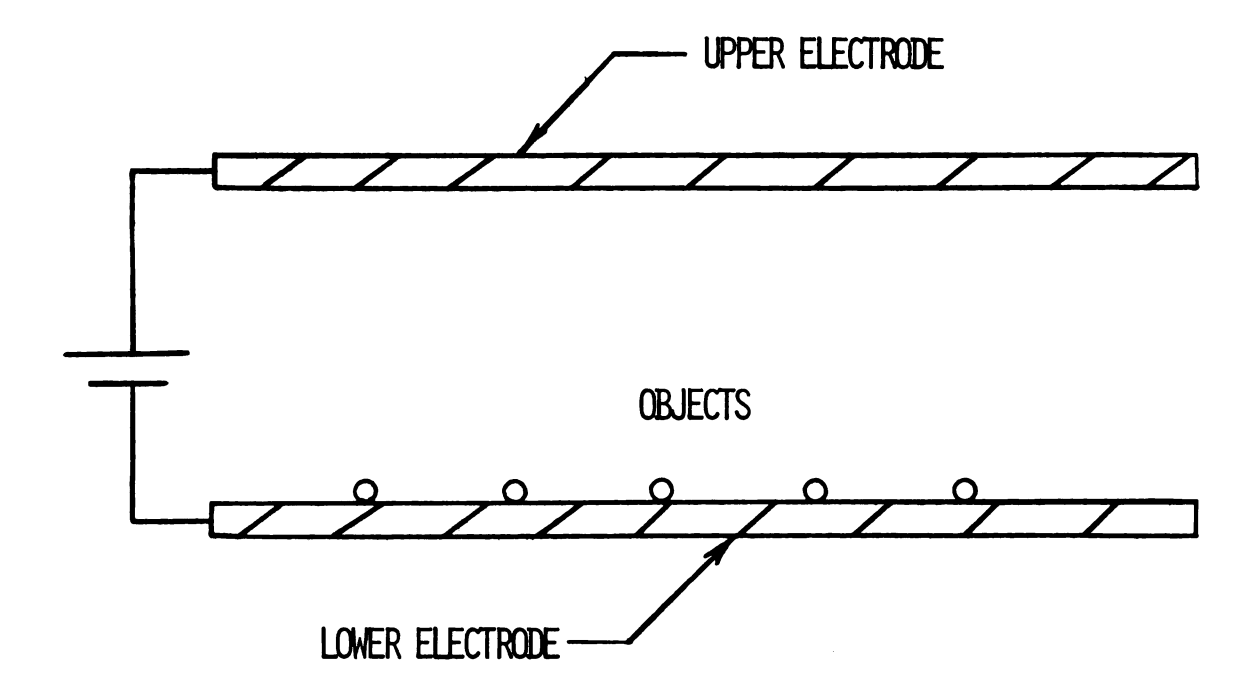


Figure 3. Schematic diagram of cell for electrostatic method.

the particle-substrate interactions arise from a smooth sphere on a smooth plane.

Trials - The cells housed either polycrystalline gold or single-crystal silver as substrates forming the lower electrode. The upper electrodes were either spherical metallic conductors (0.16 cm, 0.32 cm, and 0.48 cm-diameter) or NESA glass plates. These plates could be placed either parallel or non-parallel to the lower electrode. Analysis of data for either spherical or non-parallel upper electrodes with both (100) and (111) single-crystal silver lower electrodes indicates that the adhesion force, as measured by the electrostatic method, is approximately proportional to the square of the particle radius. This relation implies independence of electric field with respect to particle size for polycrystalline gold substrates and for single-crystal silver substrates.

With classified silver spheres (diameters < 30μ , 30μ - 45μ , 45μ - 71μ , 71μ - 100μ , and > 100μ) and NESA upper electrode separated from a single-crystal silver lower electrode by a 0.1 cm-gap, reproducible data were obtained. This indicated that the electric field strength required to overcome adhesion forces increases slightly from 4900 V/cm for 20μ -diameter silver spheres, to 6300 V/cm for spheres in the 100μ to 200μ -diameter range. Further analysis of this measuring technique indicated that the reproducibility is primarily a result of the multi-oscillations of the spheres that

first separate and then dislodge the remaining ones by impact. The spatial density of the spheres as dusted on the 0.635 cm-diameter single-crystal face range from 30 for the larger ones, to 600 for the smaller ones. Figure 4 shows a plot of removal force vs particle size as determined by the electrostatic technique.

One unexpected and unexplained, yet definite phenomenon observed is that the adhesive force, as measured by the electrostatic method in a parallel-plate air-atmosphere capacitor, is dependent on gap width, under the assumption that the force applied to a particle is proportional to the square of the applied electric field, as verified in experiments described in the Appendix. That is, as the gap is increased, the force necessary to remove large particles (greater than 100μ) decreases, whereas that necessary to remove small particles (smaller than 30μ) increases. The gap-variation phenomenon is significant enough to allow one to remove either a 200μ-diameter sphere or a 20μ-diameter sphere (both having previously been placed on the same substrate) first from the substrate. This is accomplished by keeping a constant electric field by voltage regulation and changing only the gap width.

Inconsistency of Results

The forces required to overcome adhesion for spheres on various substrates vary widely between the centrifuge method and the electrostatic method. It is hardly reasonable to

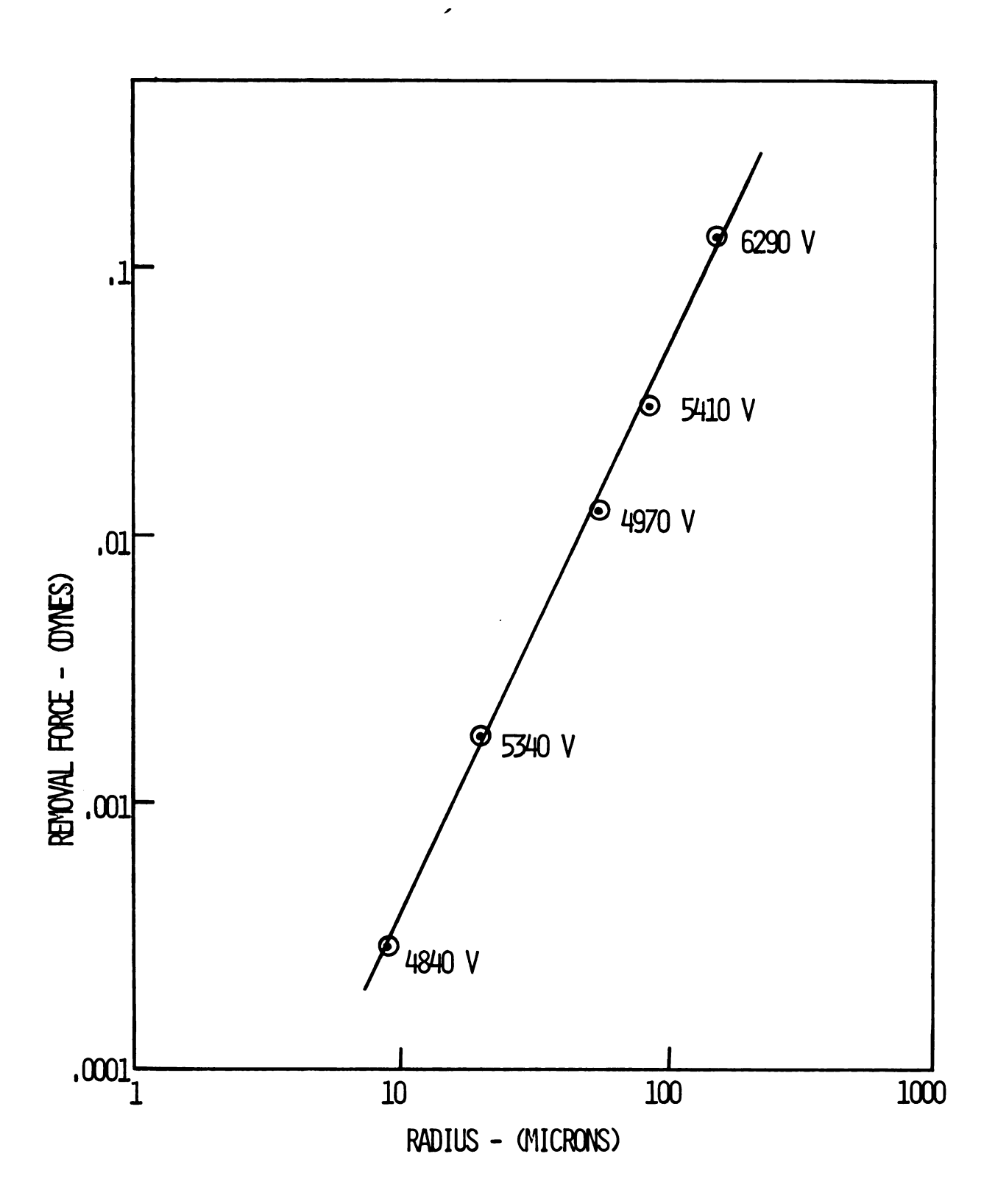


Figure 4. Electrostatic removal force \underline{vs} sphere radius for silver spheres.

assume that adhesion forces are a function of a method of measurement, and therefore that the present semi-empirical theories of solid-to-solid adhesion do not have general applicability. For small particles, <u>i.e.</u>, less than 5μ -diameter, the disparity in force measurements amounts to as much as five orders of magnitude. To reconcile these inconsistencies, we decided to study the combined effects of both electrostatic fields and normal centrifugation.

Combined Techniques

A slip-ring was built, and incorporated into the L2-65B ultracentrifuge with the Type-21 rotor. Cassettes to allow simultaneous application of electric field and centrifugal forces were made. See Figure 5 for electrical and mechanical schematic diagram. Centrifuge runs with gold spheres on polycrystalline gold substrates with an applied electric field of 10,000 V/cm (across a 0.1 cm-gap) showed a non-additive relationship between electrical forces and centrifugal forces. More precise runs with applied electric fields of 6,000, 10,000 and 12,000 volts per centimeter across a 0.1cm-gap were made in a Freon-12 (dichlorodifluoromethane -CCl₂F₂) cover gas at atmospheric pressure. This gas was chosen for two reasons, first, to increase the dielectric breakdown strength of the cover gas and thereby suppress arcing across the parallel-plate capacitor in the cassette, and second, to allow the centrifuge to attain higher speeds since Freon-12 has a lower viscosity than that of air.

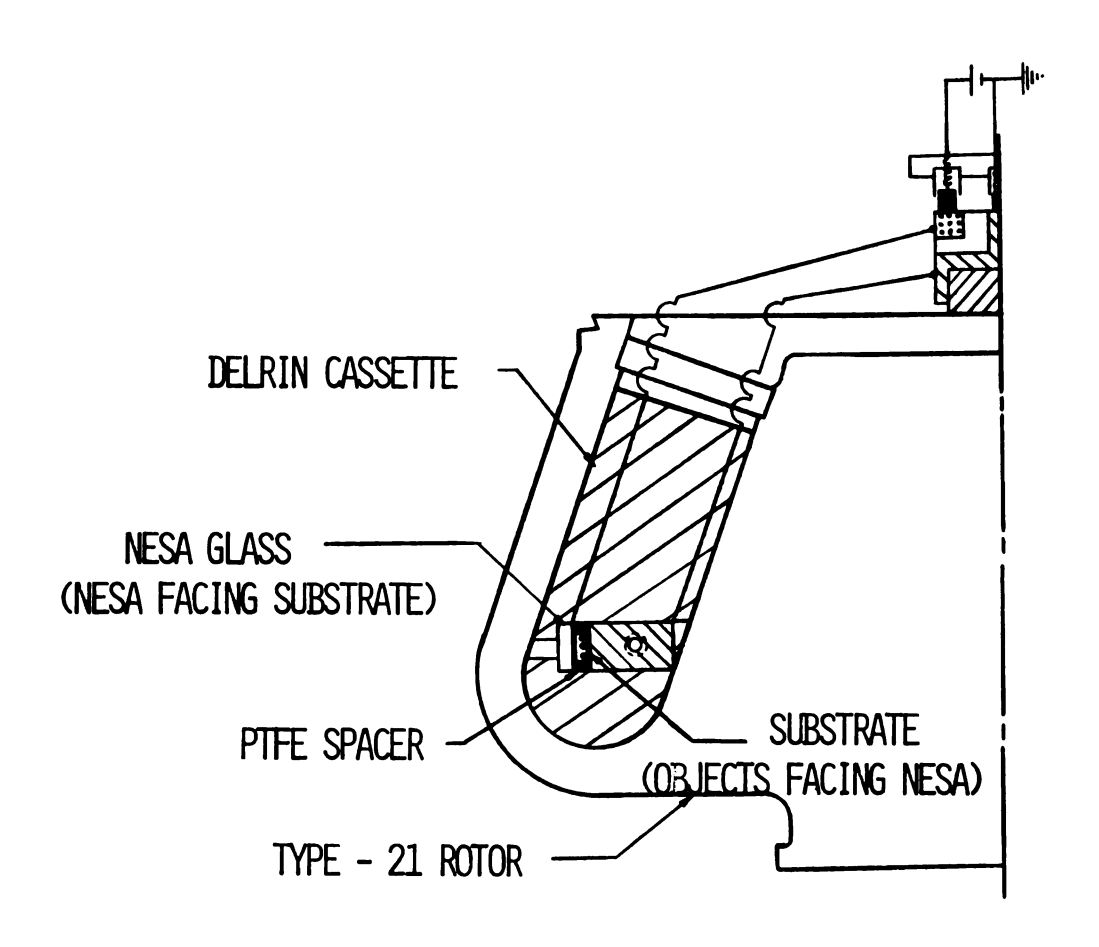


Figure 5. Schematic diagram for combined centrifugal and electrostatic method.

Qualitative results indicated that the magnitude of combined electrical and centrifugal forces necessary to break the adhesive bond is less than the magnitude of the centrifugal force required when applied alone. The predicted value of force due to the electrostatic component is only a very small fraction of the centrifuge force required for removal at the electric field strength in question. Significantly enough, the electric field strength necessary to remove particles at a 0.1 cm-gap in either Freon-12 or air is approximately 14,000 V/cm in the absence of the centrifugal force. The combined-force run yielded inconclusive results. See Figure 6 for these results along with a plot of force necessary to remove particles by the electrostatic techniques alone, i.e., at 14,000 V/cm. In light of the data obtained, additional variables must be considered to describe the mechanism of particle removal.

Surface Roughness

Two-Dimensional Model

To explain the observed anomalies in results we assume the substrate is not microscopically smooth and that some particles rest in two-dimensional grooves or vees (scratches). See Figure 7 for a schematic diagram of particle resting in a two-dimensional vee. The reaction forces are written in terms of the applied force due to either centrifugation or electrostatic fields. The F_1 and F_2 equations assume

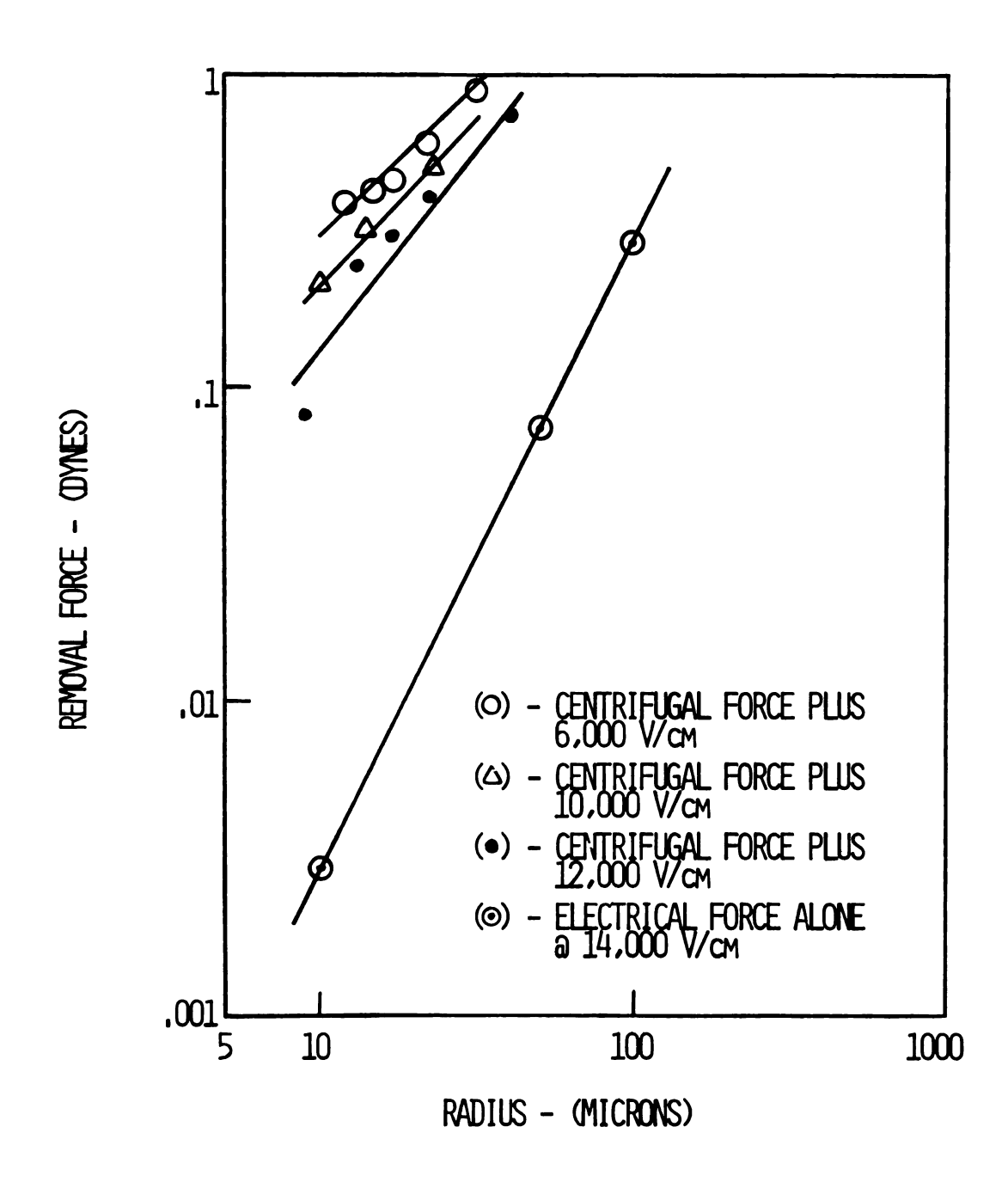


Figure 6. Removal force vs sphere radius, combined method.

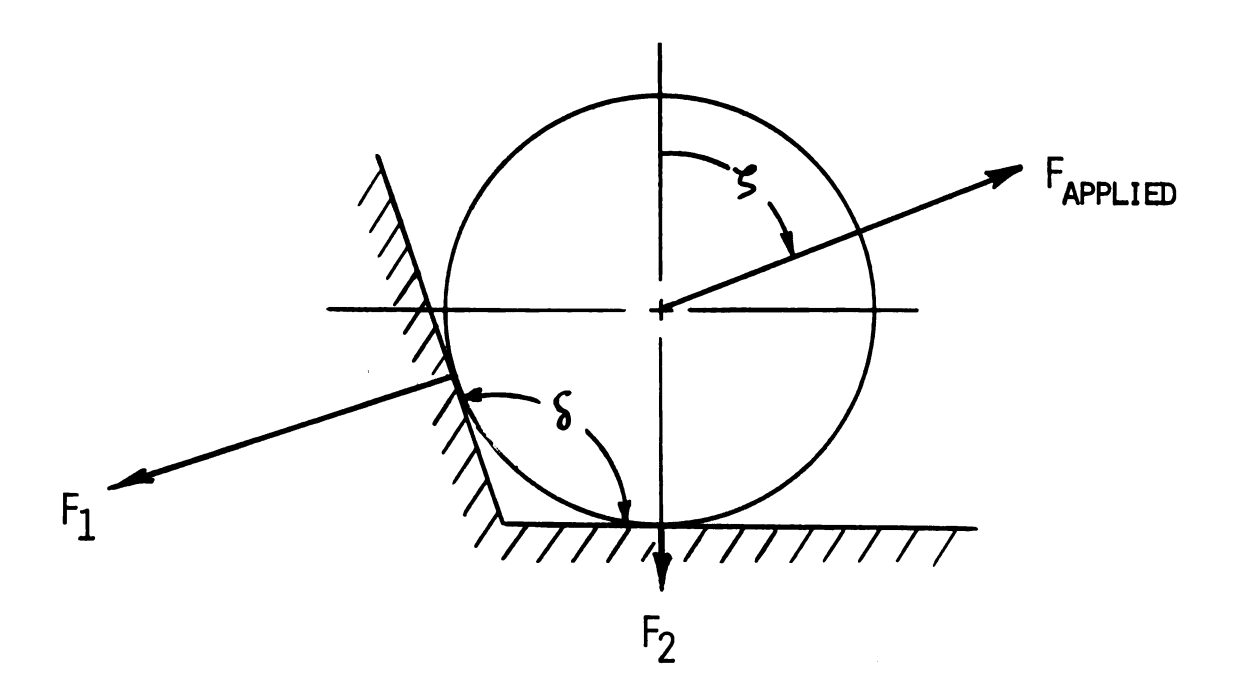


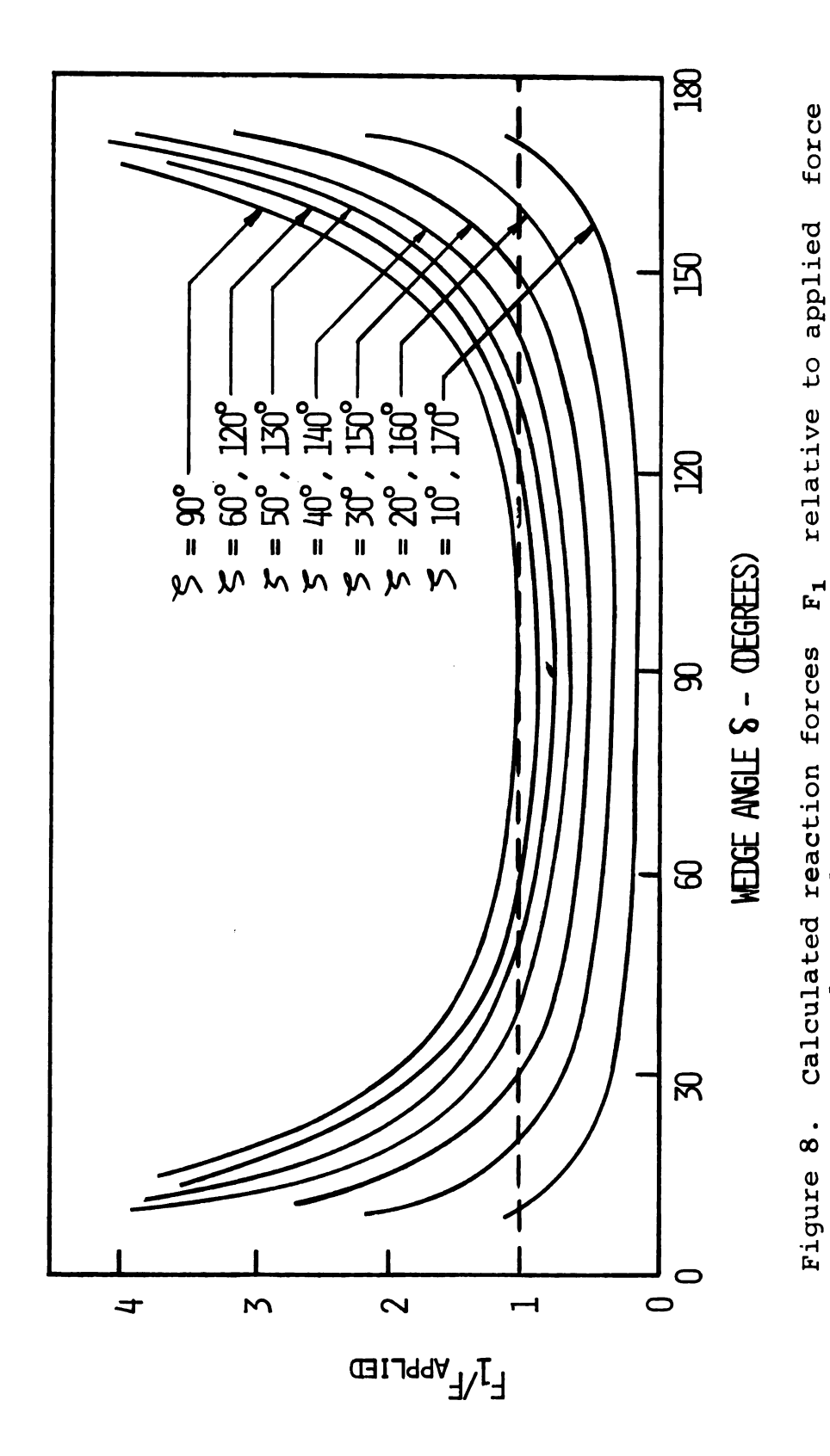
Figure 7. Sphere resting in a vee-slot.

a static rigid-body model without adhesive couples at the point of contact. Elementary statics shows that:

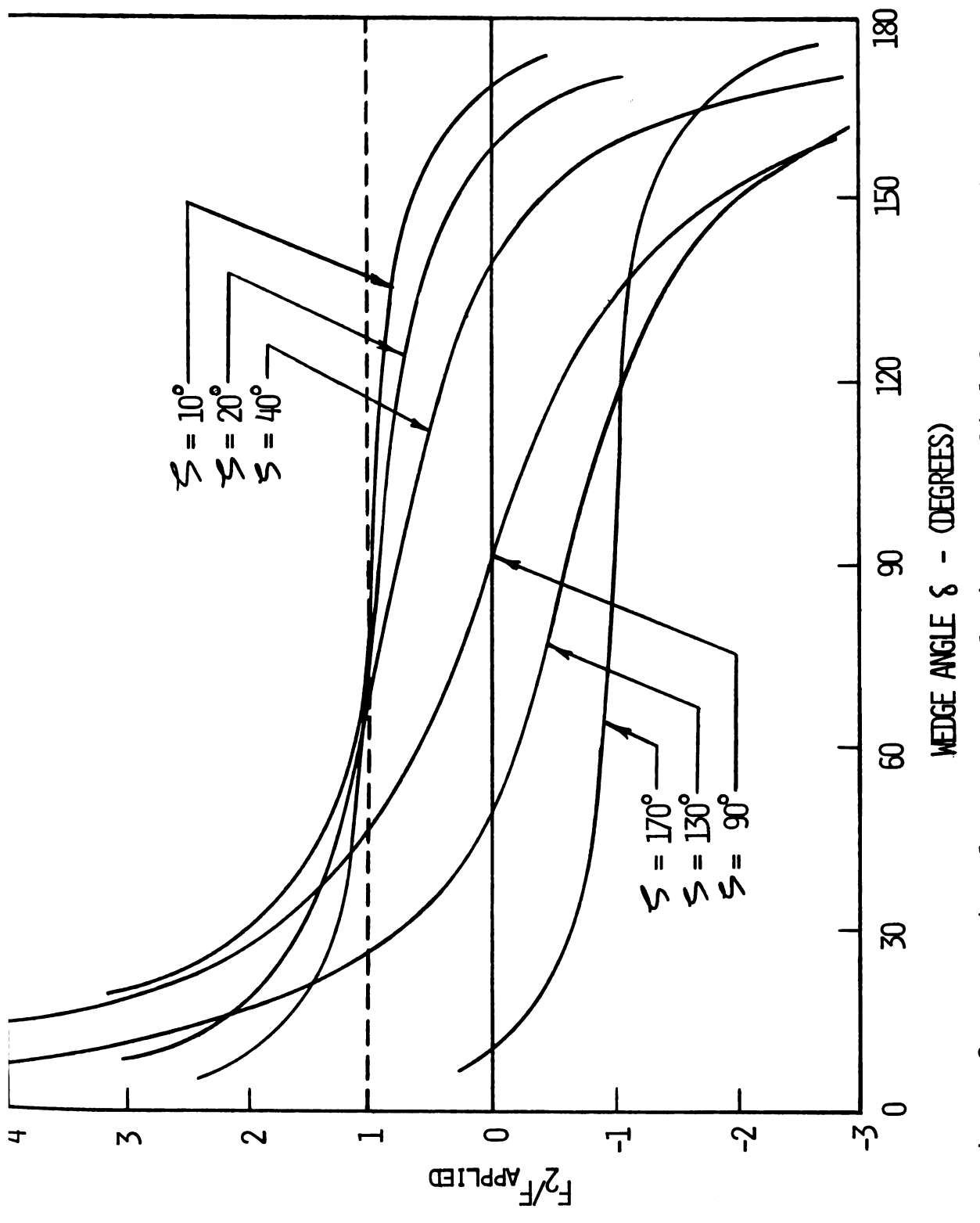
$$F_1/F_{applied} = \sin \zeta/\sin(180^{\circ} - \delta)$$

$$F_2/F_{\text{applied}} = \cos \zeta - (\sin \zeta \cdot \cos(180^{\circ} - \delta)/\sin(180^{\circ} - \delta))$$
.

A computer program yielded values of the two resultant forces in terms of the applied force for various wedge angles δ and zenith angles (. Plots of the reaction forces relative to the applied force as a function of the wedge angle are shown in Figures 8 and 9. These plots can be interpreted as follows: If either the ratio of F_1 or F_2 to $F_{applied}$ (assumed to be equal to normal removal force) is greater than unity, static equilibrium cannot be maintained. Negative values for this force ratio imply that the particle is being pressed more tightly into the substrate. The model disregards adhesive couples and/or torques that could be present at the point of contact. Centrifuge runs at various angles made later indicate that the effective force resulting from an adhesive couple is a small fraction of the normal force required to remove the particles; thus, the model is valid as a first-order approximation. This model does indicate that particles which are dusted onto the substrate into grooves or vees may be removed with a force that is significantly less than that necessary to remove particles on a smooth substrate. If one carries the model a step further and considers pyramidal or conical pits in which particles rest, the variation in applied force necessary to remove particles is only slightly modified.



vs wedge angle.



Reaction forces F_2 relative to applied force $\overline{\rm vs}$ wedge angle. Figure 9.

Electrostatic Tangential Experiments

To determine the effect of a rough substrate with an electric field applied across the parallel-plate capacitor with conductive particles resting on the electrode, the following experiment was conducted. Two large conductive spheres were placed on the lower electrode of a 5.08 cm-gap parallel-plate capacitor. One sphere was 3.78 cm in diameter, the other 0.87 cm in diameter. The spacing between the two spheres was initially set at 0.635 cm. The potential from a DC power supply was increased slowly from zero to approximately 6000 V DC, at which voltage the spheres separated by rolling apart. The experiment was repeated by replacing the 0.87 cm-sphere with a second 3.78 cm-sphere. Again, the spheres separated upon increasing the potential. We believe that these scaled-up models represent the behavior of a small gold sphere near a surface protuberance, or of two spheres near each other. Evidently the application of an electric field across a parallel-plate capacitor does not remove small spheres from apparently smooth substrates by pulling them away perpendicularly, as is customarily assumed. In other words, particle-substrate and particle-particle interactions evidently produce tangential forces on spheres when they are placed in an electrostatic field perpendicular to the plane substrate on which the spheres rest.

Centrifuge Zenith Angle Evaluations

From the results obtained by the electrostatic method, the centrifuge technique with normal forces, and the results for combined forces, we decided to determine rigorously the magnitude of force acting through the center of gold spheres at various zenith angles as a function of the radius of the sphere for substrates of various hardness.

Apparatus

The centrifuge was operated with a modified cassette inserted in the rotor tube bores of the Type-21 rotor. cassette to house substrates and spherical gold objects consisted of two half cylinders, one with a 1.27 cm-diameter spot face, the other with a 0.635 cm-diameter hole through the cylinder perpendicular to the flat side so that microscopic observations could be made. The substrate is placed on the spot face, opposite the 0.635 cm-diameter hole in the opposing half cylinder. The half cylinders were fastened together with screws and inserted in a Delrin cassette machined to fit in the Type-21 rotor tube bore hole. A set screw was provided to allow the zenith angle to be varied from 0 to 2π radians (see schematic in Figure 10). With this arrangement, runs at a zenith angle of 0^{0} would apply only removal forces as in the traditional centrifuge runs, whereas runs at a zenith angle of 90° would apply only a couple. Values of zenith angles between 00 to 900 would apply a combination of tangential and normal forces.

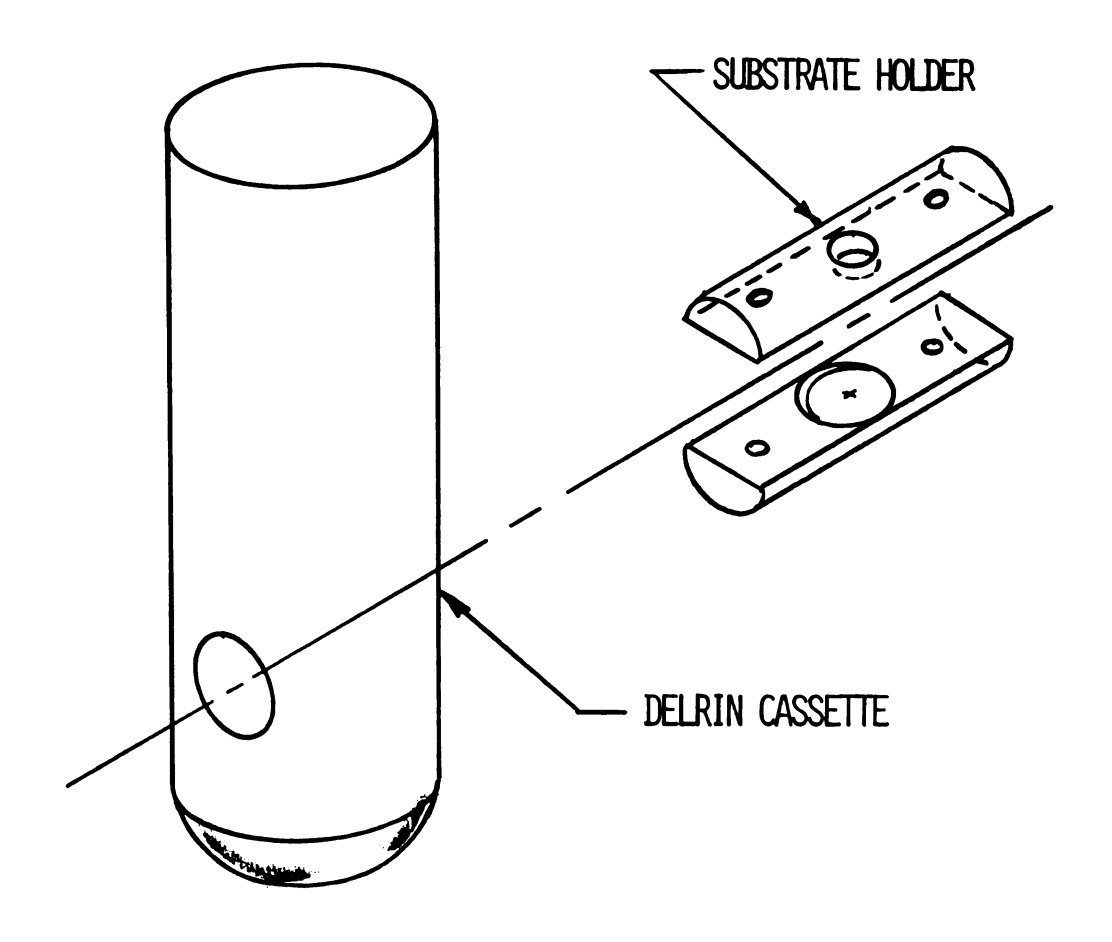


Figure 10. Schematic of cassette for zenith angle centrigugal runs.

Adherents

The materials in the gold-on-gold experiments consisted of the previously-described spheres on substrates prepared in the following manner. Kimble Exax No. 1 cover glass slides were first vacuum deposited with iron (for better film adhesion), and this vacuum deposited with gold 10^{-4} cm thick. The resulting surface was of optical quality, <u>i.e.</u>, the surface roughness was less than 0.25×10^{-4} cm.

Experimental Results

Centrifuge runs were made for gold particles ranging from 10μ to 60μ in diameter as a function of zenith angle at steps of 30° . Contrary to our expectations, we found a novel phenomenon for gold on gold, as seen in Figure 11. Here the force of removal is plotted against zenith angle for particles of various sizes. For zenith angles greater than 90° , the applied force necessary for particle removal actually decreased to a minimum at approximately 120° and then rose steeply as the zenith angle approached 180° . Figure 12 shows the dependence of applied force for removal on particle size for runs at various zenith angles.

The same set of experiments was completed on a 1.27 cm-diameter 0.013 cm-thick optically polished nickel substrate. Here the removal force increased past the sub-minimum (ζ = 90°) to a sub-maximum (ζ = 120°) and at approximately 150° then decreased to a minimum, actually below that of 90°, and then rose steeply (see Figure 13). We conjecture that

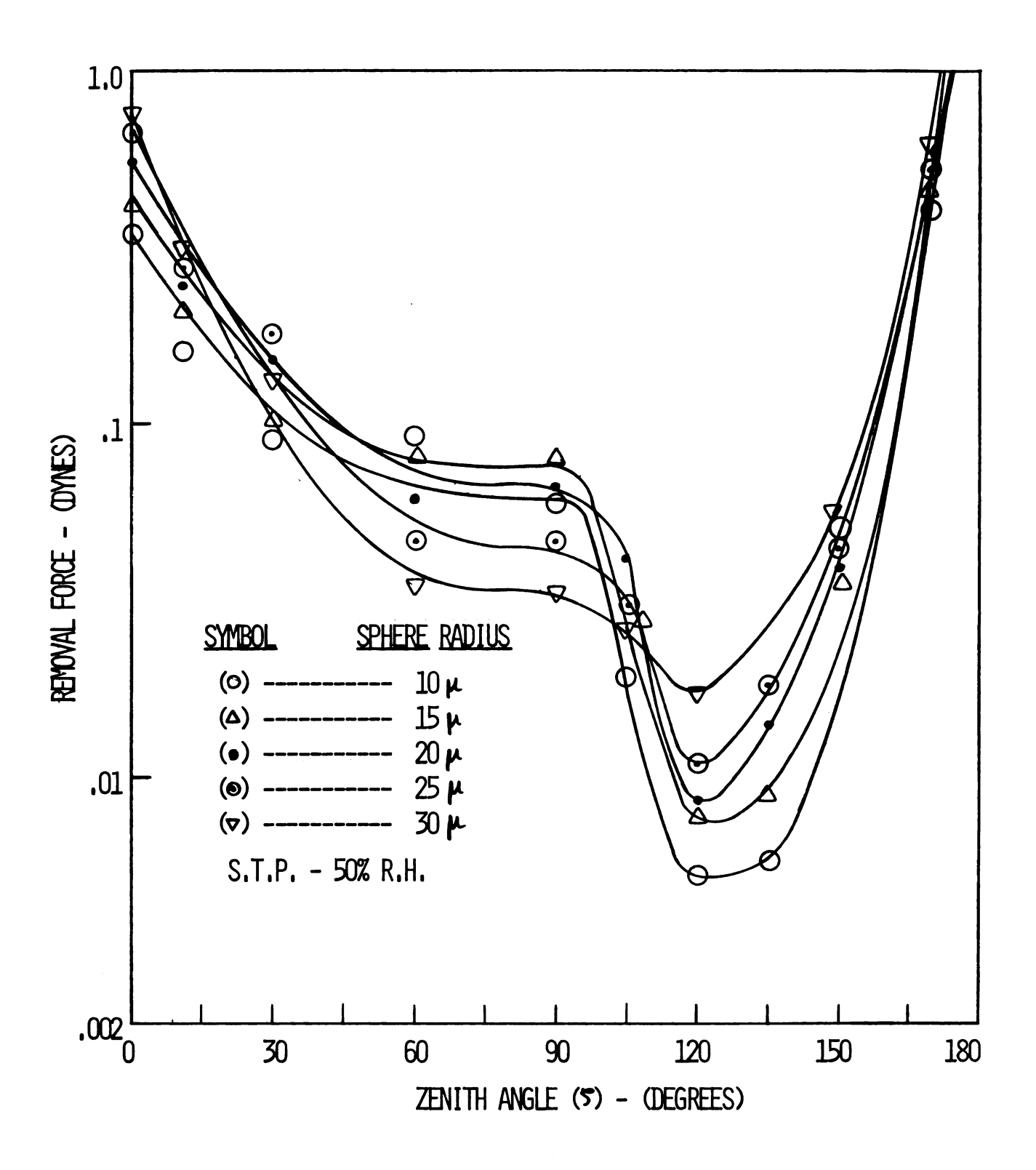


Figure 11. Centrifugal removal force vs zenith angle for various radii gold spheres.

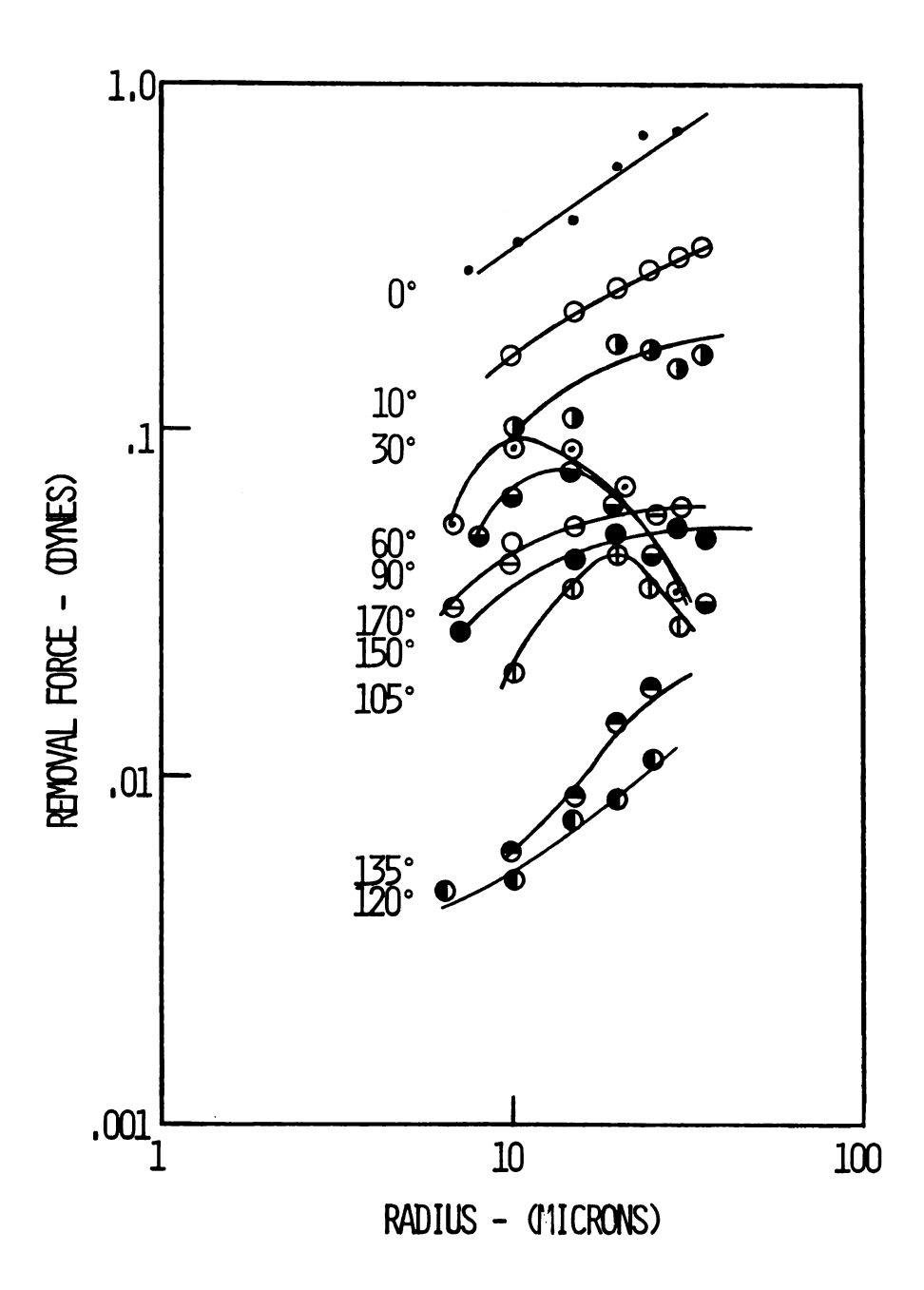


Figure 12. Centrifugal removal force \underline{vs} sphere radius at various zenith angles.

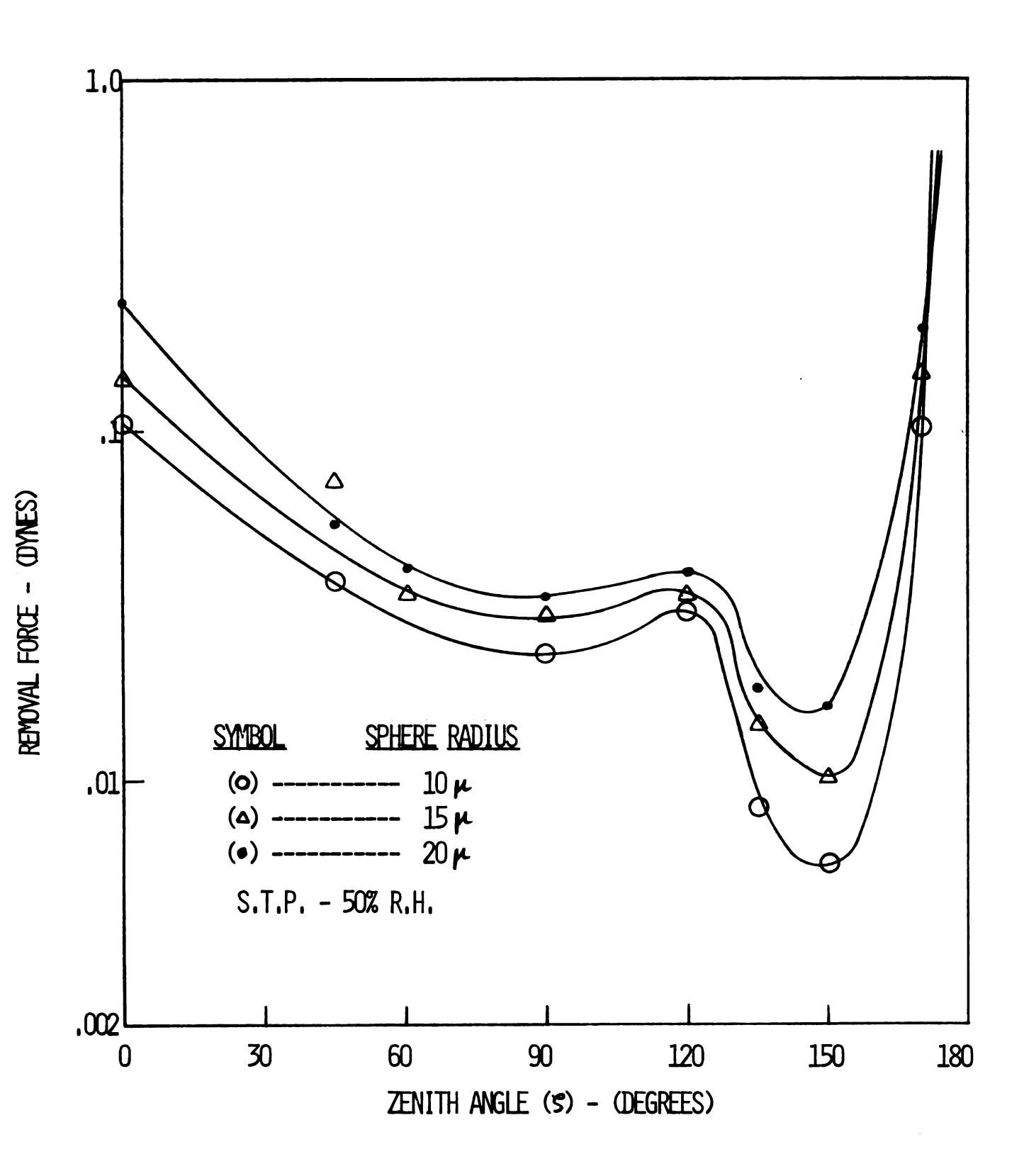


Figure 13. Centrifugal removal force \underline{vs} zenith angle for various radii gold spheres.

in this case the yield point of the substrate material (at the contact points) was not exceeded significantly until $F_{applied}$ · cos ζ plus the adhesive force became sufficiently large. This relation occurred at approximately ζ = 120°. Figure 14 shows a plot of the removal force \underline{vs} particle size for gold spheres on a nickel substrate with zenith angle as the parameter.

Exploratory experiments were conducted with gold and silver spheres on stainless-steel polished substrates. In these cases, the minimum force, as a function of zenith angle, was obtained at 90°. The resulting curve for force vs zenith angle was asymmetric about the 90° point, the curve rising more sharply at larger angles. Other experiments with silver spheres on gold substrates yielded curves similar to those for gold on gold. The same result held for both gold and silver spheres placed on lead-tin alloys.

Discussion of Experimental Results

The data in Figures 11-14 were obtained with optically smooth substrates, that is, having asperities far smaller than the particle size. With substrates having a surface roughness approaching that of the particle size, an obvious dispersion in data appeared. Generally, the spheres tended to be removed with smaller applied force for either small zenith angles or for large zenith angles, as compared with runs made on smooth substrates. Moreover, removal forces from rough substrates were larger than from smooth substrates

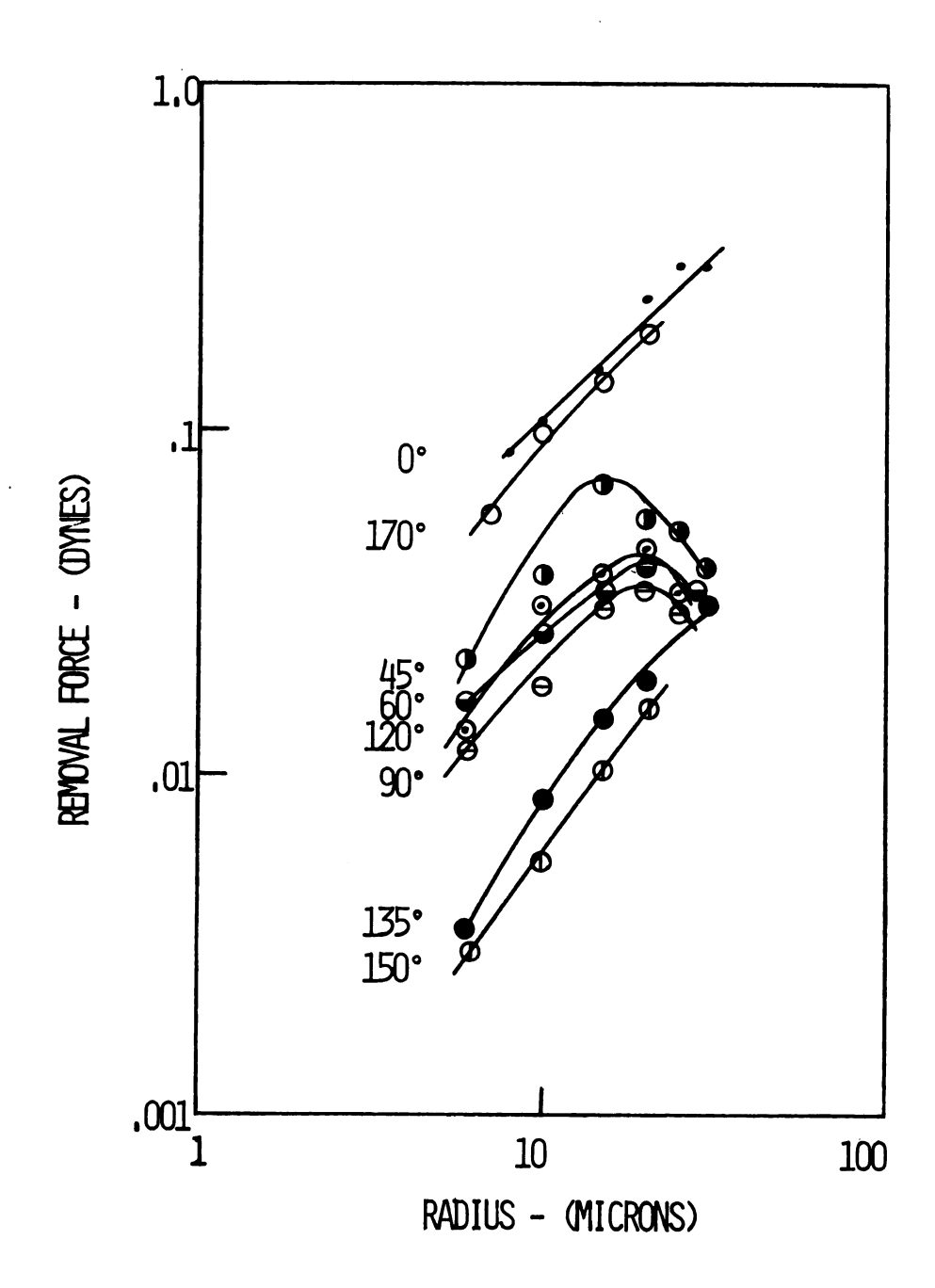


Figure 14. Centrifugal removal force \underline{vs} sphere radius at various zenith angles.

when a zenith angle that yielded minimum removal forces was used, <u>i.e.</u>, in the case of a very hard substrate $\zeta = 90^{\circ}$ and for softer substrates $\zeta = 120-150^{\circ}$. Zenith-angle runs at a pressure of 10^{-3} mm Hg, in air, and in a Freon cover gas did not alter the removal forces within the experimental error involved in the centrifuge technique. Nor did the value depend on the duration of the adhesion. Centrifuge runs generally lasted 300 seconds; to see if duration of application of applied forces affects removal force, the centrifuge was run at a given speed for 10^{5} seconds without any additional particles being removed.

Values plotted on Figures 11-14 were obtained with 50 to 500 particles on a given substrate. The points are unweighted averages of removal force derived from a computer program for the various densities, particle sizes, rotor radius arm, and speeds.

Particles were grouped into five micron classes with their associated minimum and maximum removal speeds. Average removal force and particle size were determined for each class at a given zenith angle.

Particle sizes were individually obtained within 1μ by scaling the photographs, the microscopic and photographic magnification being previously calibrated. Any possible discrepancy between the density of the samples and those listed in standard handbooks are so small that the latter were adopted. The rotor radius arm had a maximum variance of \pm 2%, depending on zenith angle employed. Zenith angle placement was accurate within \pm 1° .

Interpretation of Results

In the evolution of our study the critical point was the realization that the separation process was in almost all cases controlled by the tangential forces. It will be recalled that we reached this conclusion when the electrostatic removal forces turned out to be much lower than expected.

We seek an explanation for dependence of removal force on zenith angle. An adhesive force alone acting through the point of contact cannot explain the observed dependence since even the slightest tangential force would produce a couple sufficient to remove the particle. Consequently we were led to represent the contact as a distributed load, simulating it by an adhesive force \mathbf{F}_{R} and an adhesive couple \mathbf{N}_{R} , as seen in Figure 15.

For the conditions of particle removal, we first assume that the particle will slide off when the tangential component of the applied force exceeds a limiting value F_t^* , or will be pulled off when the normal component of the applied force exceeds a limiting value F_n^* , or will roll off when the applied couple exceeds a limiting adhesive couple N*. The value F_n^* can be obtained experimentally from observing the removal force F_R (0°), where the tangential component vanishes. The value of F_t^* can be obtained experimentally provided the particle slides off, by observing the removal force F_R (90°), where the normal component vanishes. The value of N* can be obtained in

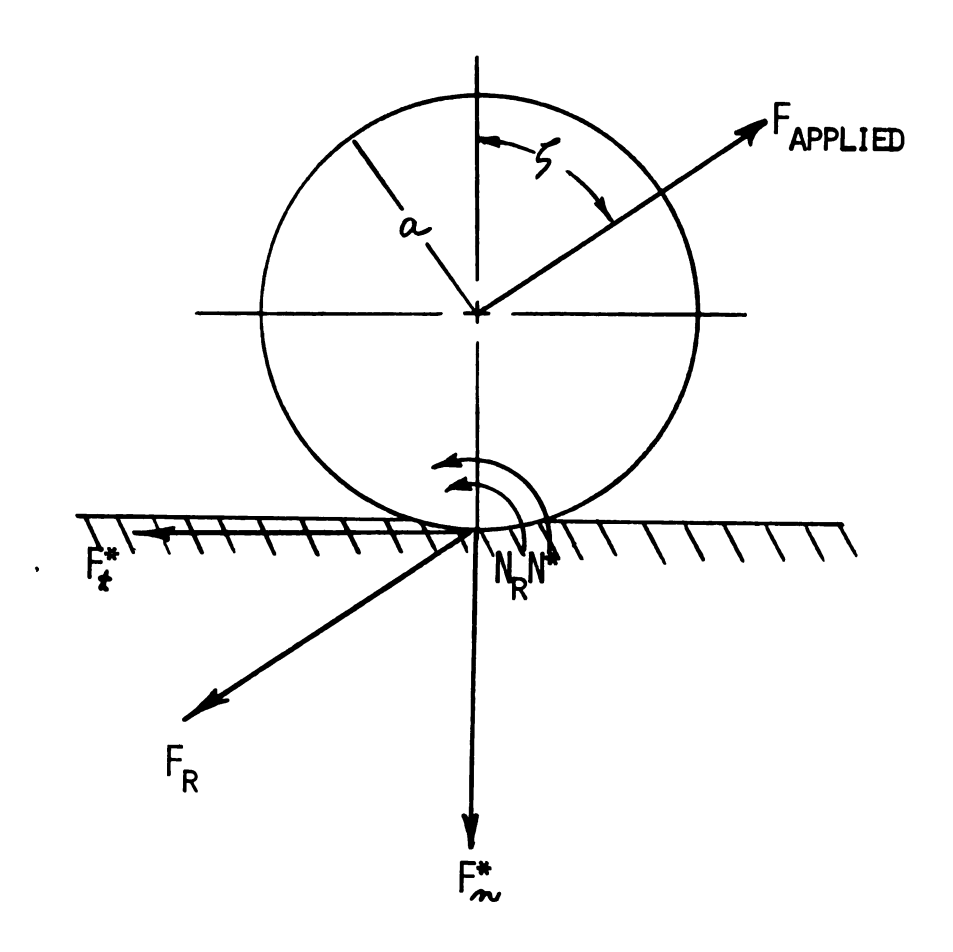


Figure 15. Model for sphere on plane.

the same sort of experiment provided the particle rolls off. The conditions for particle removal (instability criteria) will then be the following for the entire range of zenith angles from 0° to 180° .

Case I.- $\zeta < 90^\circ$

- a. Force limited
 - 1) $F_{applied} \cdot \sin \zeta > F_{t}^* \text{ (slid off)}$
 - 2) $F_{applied} \cdot \cos \zeta > F_n^*$ (pulled off)
- b. Couple limited
- 1) $F_{applied} \cdot \sin \zeta \cdot a > N^*$ (rolled off) Case II.- $\zeta \geqslant 90^0$
 - a. Force limited
 - 1) $F_{applied} \cdot \sin \zeta > F_{t}^{*}$ (slid off)
 - b. Couple limited
- 1) $F_{applied} \cdot \sin \zeta \cdot a > N^*$ (rolled off) Case III.- Combination of the above.

Let us assume that the adhesive couple N* is not exceeded; then the applied force necessary for particle removal in the "pulled off" mode is proportional to the removal force, F_R (0°) or F_n *, times sec ζ . The applied force necessary for particle removal in the "slid off" mode is proportional to the removal force, F_R (90°) or F_t * times csc ζ . This relation is valid only if F_t * is independent of the normal load. Figure 16 shows the normalized removal force as a function of zenith angle under the conditions described with F_t */ F_n * = 0.1, under the assumption that N_R < N*, and that there is no interdependence between the criteria for removal.

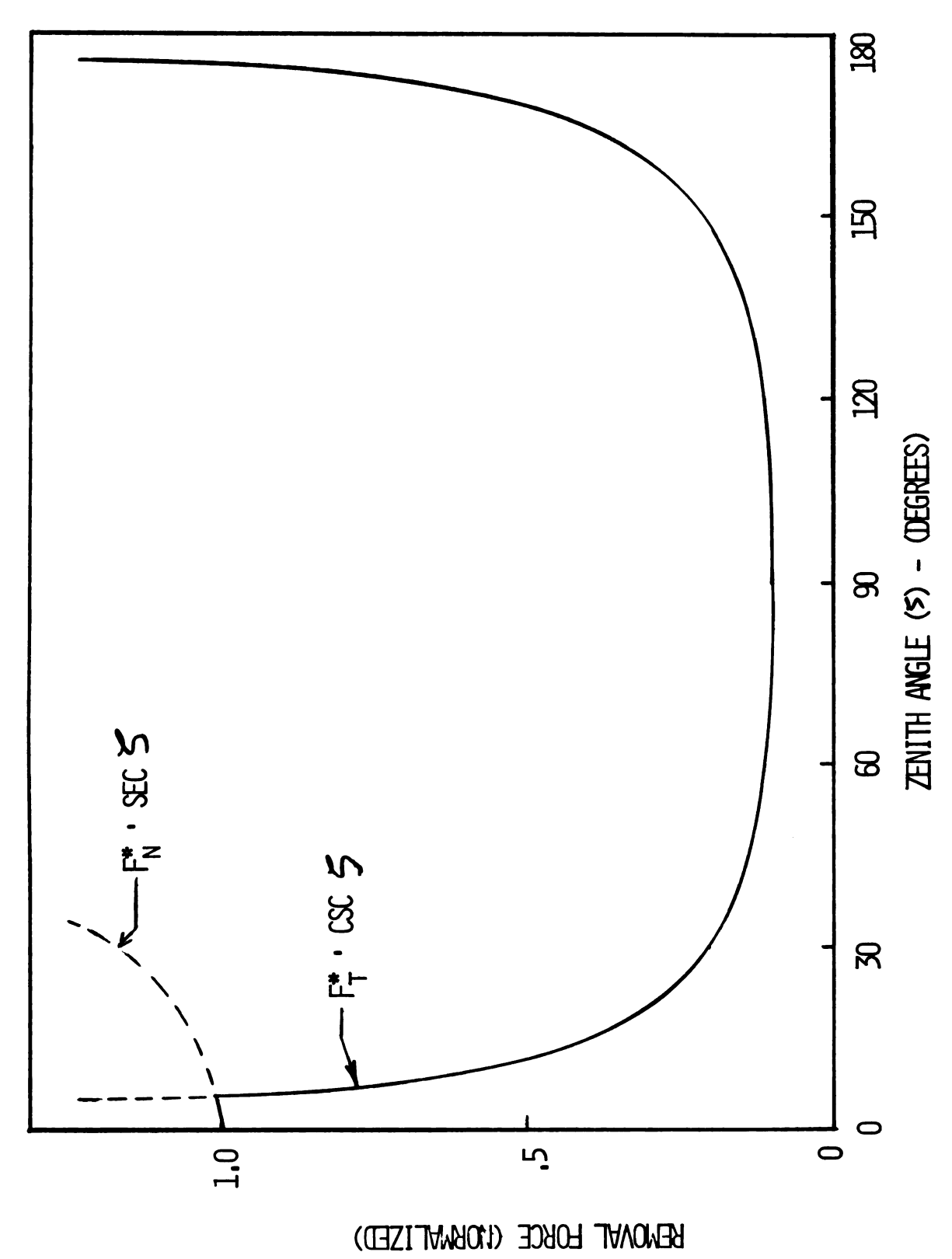


Figure 16. Normalized sliding and pulling removal force vs zenith angle.

For particles to be "rolled off" it is only necessary that N* be exceeded. The applied force necessary for particle removal in this mode is proportional to the removal force, F_R (90°) or N*/a, times csc ζ -- precisely the same as in the "slid off" mode. This relation is valid only if N* is independent of the normal load.

It is, of course, unrealistic to take the critical couple -- which is supposed to arise from the distributed load -- as independent of normal force. To refine our model somewhat we assume that N* can be described by a generalized law of rolling friction[‡] of the form:

$$N^* = akw^n/(2a)^m$$
.

Here k is a coefficient of rolling friction and n and m are parameters; the relation will be useful only if all three quantities prove to be reasonably constant over the range of experiments of interest. W, the normal load, is taken to be F_n^* minus the normal component of $F_{applied}$ for $\zeta \leq 90^\circ$, and F_n^* plus the normal component of $F_{applied}$ for $\zeta \geq 90^\circ$.

The effect of the dependence of N^* on the normal force is shown in Figure 17 for a particle of fixed diameter and n = 0, 1/2, 1, 2. For n > 0, the limiting couple

$$F_{\text{rolling}}^* = N^*/a = k w^n/D^m$$

[†]This law is obviously a form of

where F^{*}_{rolling} is the force necessary to roll a sphere of diameter D on a plane, the force being applied parallel to the plane through the center of the sphere.

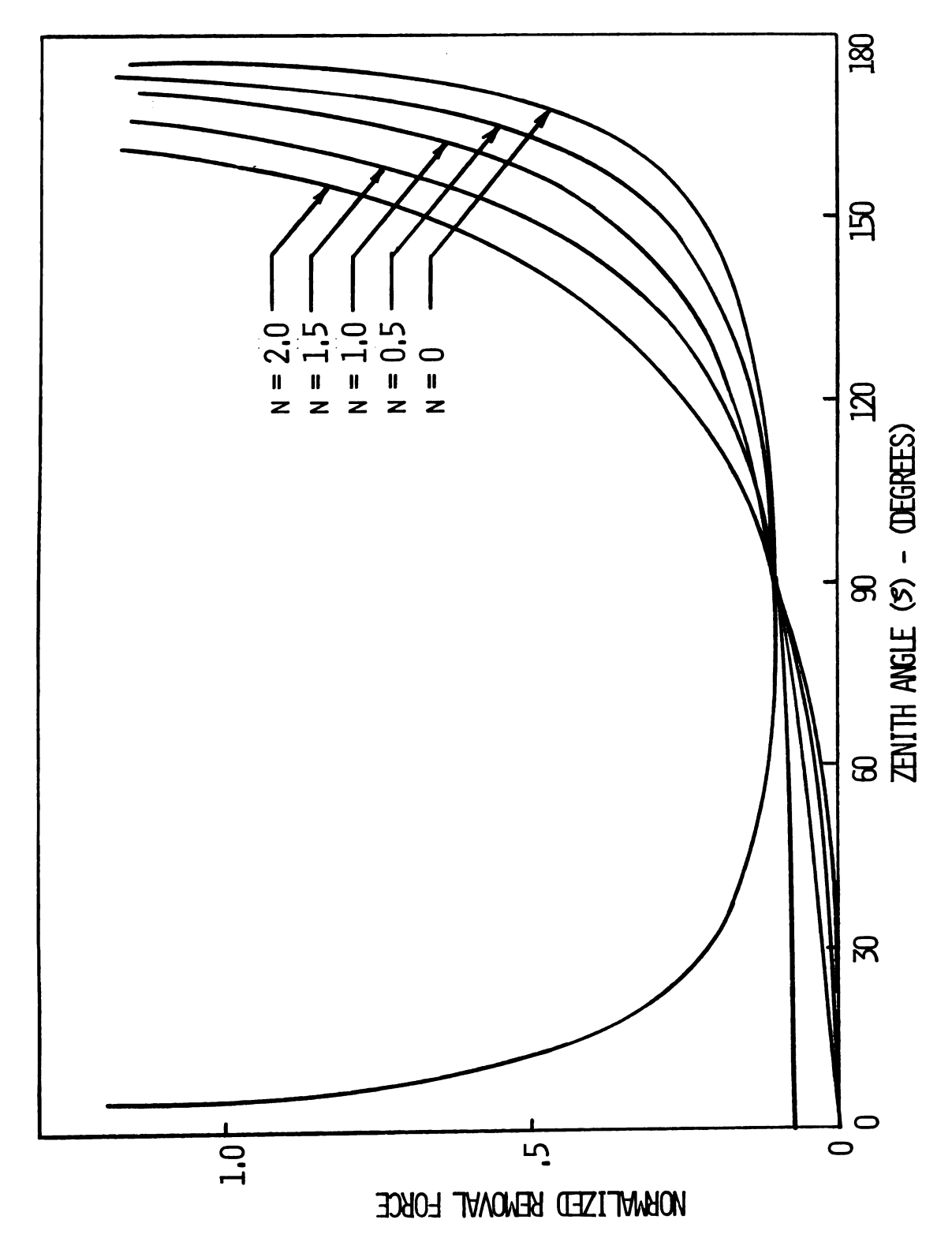


Figure 17. Normalized rolling removal force vs zenith angle.

increases over the value for n=0 at $\zeta > 90^{\circ}$, as the normal force presses the sphere into the plane; the action is reversed for $\zeta < 90^{\circ}$. This effect appears in the asymmetry of these curves. For the normal load in the sliding case previously discussed, the normalized removal force is the same as in the rolling case for n = 1 as shown in Figure 17. Comparison of the experimental curves with the previous sliding and pulling curves, the modified sliding curve (n = 1), and the rolling curves for n > 1 suggests that for $\zeta < 90^{\circ}$ particles are removed either by pulling at very small angles, or by sliding or rolling at larger angles, though not according to the conventional laws of rolling and sliding friction. On the other hand, for ζ > 900, the upward trend of the curve shows that sliding or rolling are possible mechanisms of removal for hard substrates. This explanation must be refined in the case of soft substrates, however, in view of the shift of the observed minimum past 90°.

In seeking to refine the model, let us estimate the stress distribution around the interface to see whether plastic deformation occurs under the assumption that values for macroscopic mechanical properties hold for the microscopic regions in the neighborhood of contact. The most readily interpretable mode of separation is removal at $\zeta=0^{\circ}$, where N_R vanishes and only F_R need be considered. If the compressing force between the sphere and the plane is taken to be equal to the observed force required to remove

the sphere, namely F_n^* , the calculated maximum contact pressure — as estimated by Hertz's formulas for pressure between curved objects — exceeds the compressive strength of gold by a factor of two (10 μ -radius gold sphere on a plane gold substrate). Therefore plastic deformation should occur, the particles welding to the substrate in the center of the contact area. In such cases the tensile strength of the interfacial bond will then be equal to that of the weaker adherent.

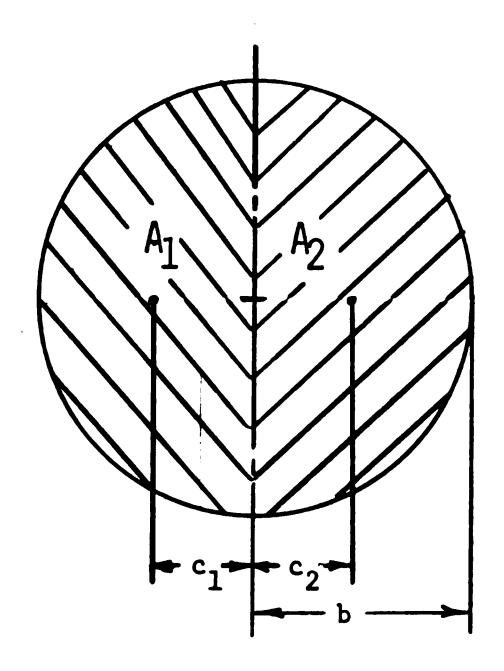
For removal by pulling at angles other than 0^{0} , we assume that this criterion will still be valid. The calculation of the stress in the interfacial region becomes complicated, however, by the appearance of the couple N_p as well as the force F_R . An accurate calculation of the stress distribution is difficult even for the case of purely elastic deformation, and in the case at hand is unattainable without detailed knowledge of the regions of plastic and elastic deformation. Hence we simulate the actual distribution by assuming a stress distribution resulting from superimposing a stress $\bar{\sigma}_{_{\mathbf{U}}}$ set up by the applied force onto a stress distribution $\bar{\sigma}_{_{11}}$ set up by the applied couple. The stress $\bar{\sigma}_{v}$ is taken to be uniform over the entire circle of contact of radius b. It will be compressive or tensile according to the sense of the normal component of the applied force, that is, compressive when Fapplied sphere into the plane, tensile otherwise. The stress $\bar{\sigma}_{_{11}}$ is taken to be uniform over each of two segments of the circle of contact, compressive over one part, tensile over the

other, as the sphere tends to rotate about some chord of the circle of contact that is perpendicular to the line of action of the force. This concept may perhaps become clearer upon examination of Figure 18, in which the chord happens to be the diameter dividing the circle of contact into area A_1 over which the stress $\bar{\sigma}_{\mu}$ is directed downward (tensile), and the area A_2 over which it is upward (compressive).

To treat the matter quantitatively, we note that F_n , the normal component of the reaction force F_R , must equal the stress $\bar{\sigma}_V$ times πb^2 , the area of the circle of contact, that is,

$$F_n = F_R \cos \zeta = F_{applied} \cos \zeta = \bar{\sigma}_v \pi b^2$$
.

We note next that F_t , the tangential component of the reaction force, times the moment arm a, must equal the torque set up by the stress $\bar{\sigma}_{\mu}$ acting over the areas A_1 and A_2 , each equal to $\frac{1}{2} \pi b^2$. The torque from the former is the force $\bar{\sigma}_{\mu}$ A_1 times the lever arm $4 \ b/3\pi$, the distance of



CIRCLE OF CONTACT

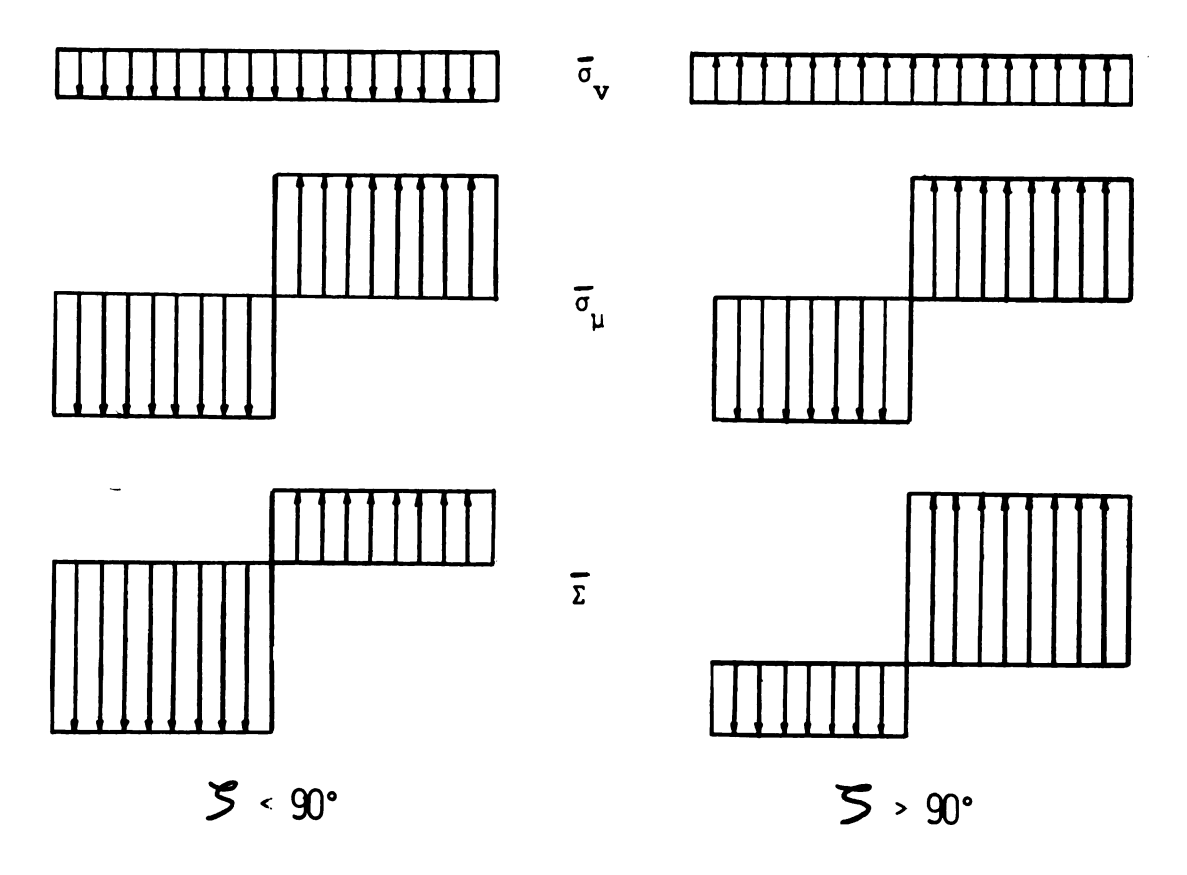


Figure 18. Uniform stress distribution resulting from applied force.

the centroid of A_1 from the assumed line of incipient rotation, namely, the diameter shown. Because of symmetry, the torque from the stress over A_2 has the same value as that from the stress over A_1 . Hence we may write

$$F_t$$
 a = aF_R sin ζ = $aF_{applied}$ sin ζ = $2 \cdot \bar{\sigma}_{\mu} \cdot \frac{1}{2} \pi b^2 (4b/3\pi)$

The total stress $\overline{\Sigma}$, the sum of the two stresses just calculated, is then:

$$\bar{\Sigma} = \bar{\sigma}_v + \bar{\sigma}_\mu = (F_{applied}/\pi b^2) [\cos \zeta \pm (3\pi a/4b) \sin \zeta].$$
 These relations have been illustrated in Figure 18.

Removal occurs when the effective interfacial tensile stress exceeds the tensile strength of the weaker adherent, if the shear stress $F_{\rm t}/\pi b^2$ is ignored. The values of $F_{\rm applied}$ required to meet this criterion are plotted as the top curve of Figure 19. Here the values have been normalized by dividing by the stress at $\zeta=0^{\rm o}$, namely, $F_{\rm applied}/\pi b^2$. The ratio $3\pi a/4b$ has been set equal to 10, a reasonable value in view of the experimental findings on removal force at $0^{\rm o}$ and $90^{\rm o}$.

The top curve in Figure 19 displays many of the properties of the curves obtained experimentally. But it does not show the dip at zenith angles past 90° . To provide for such a prediction, we relax the condition that the sphere tends to rotate about a diameter. Instead we assume that the chord of rotation is shifted to the left a certain fraction of the radius b, as shown in Figure 20. The areas A_1

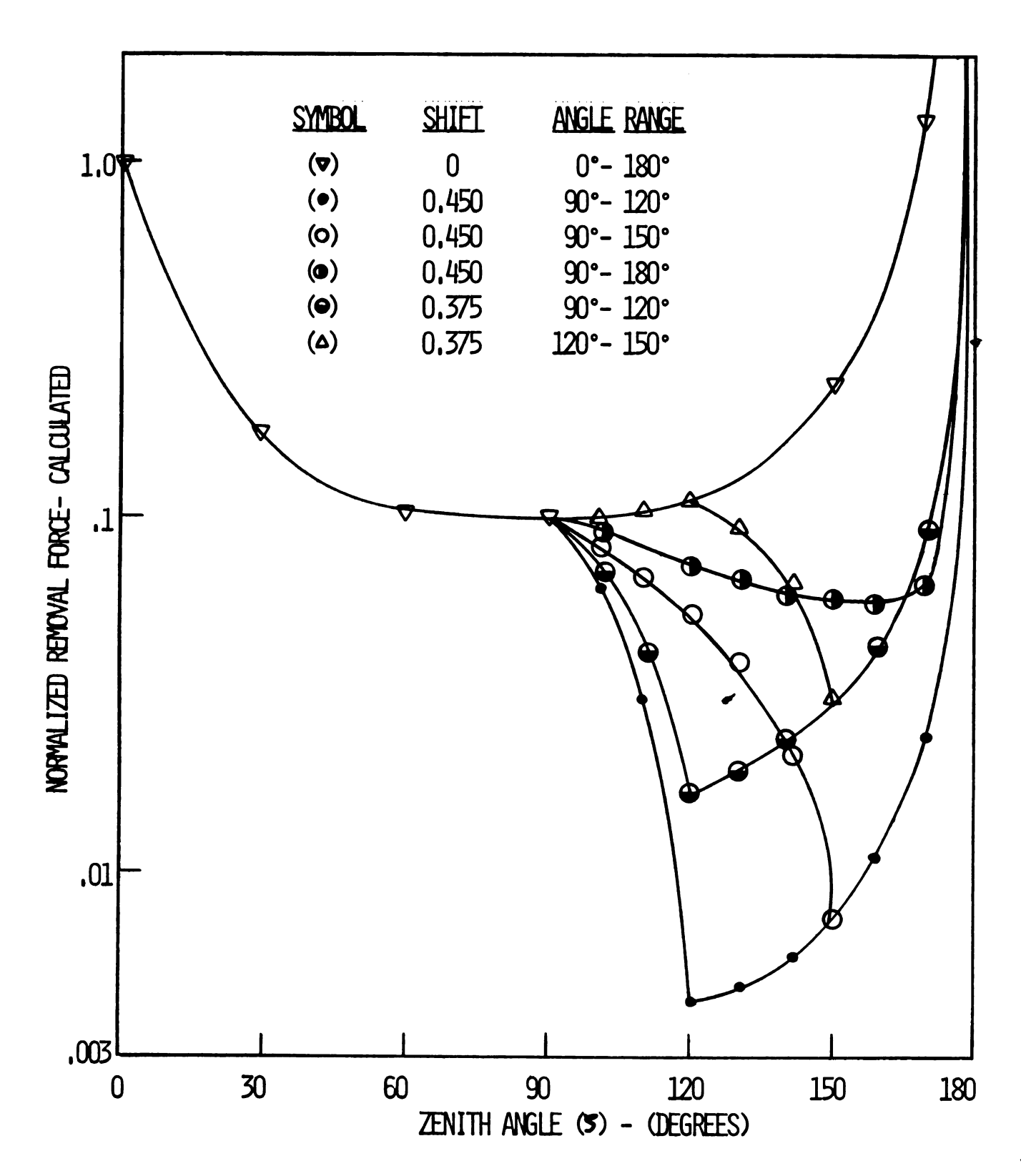


Figure 19. Normalized removal force <u>vs</u> zenith angle for shift of center-of-rotation.

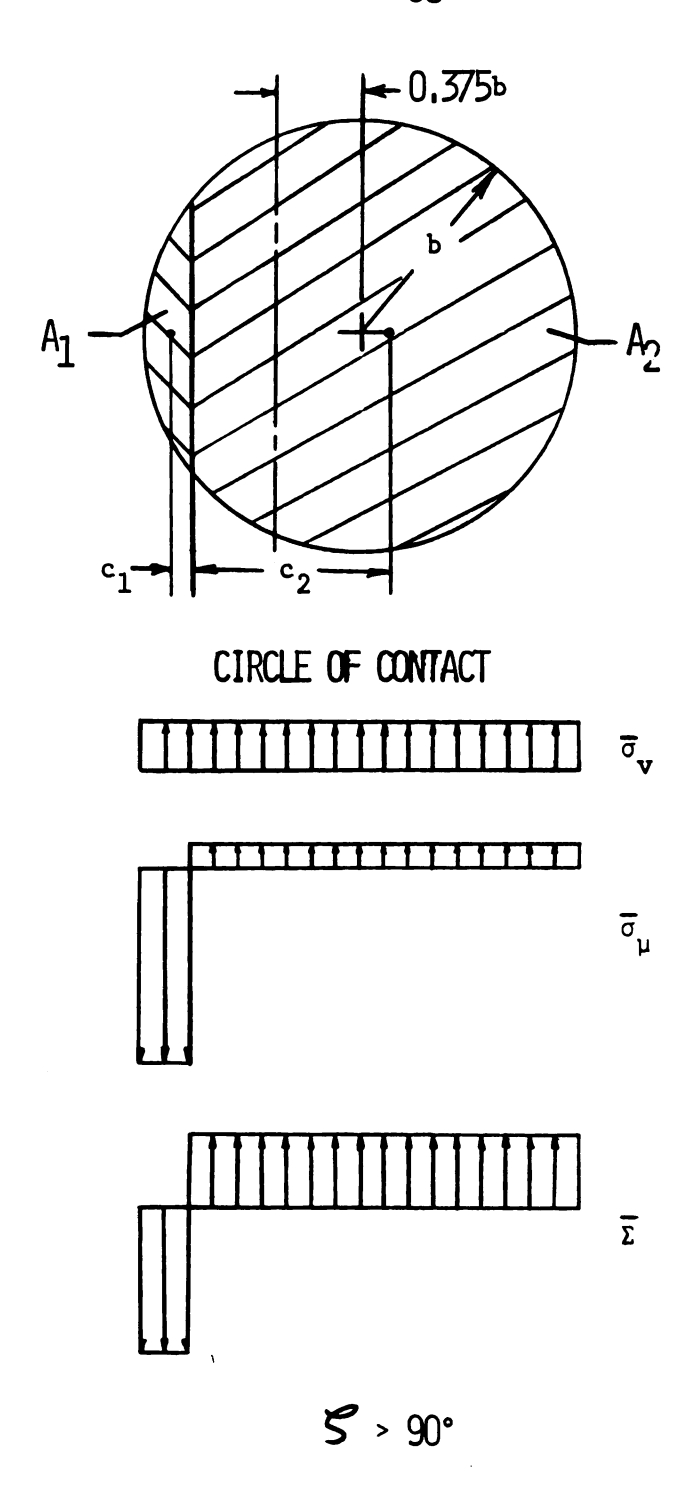


Figure 20. Uniform stress distribution resulting from applied force and 0.375b shift in center of rotation.

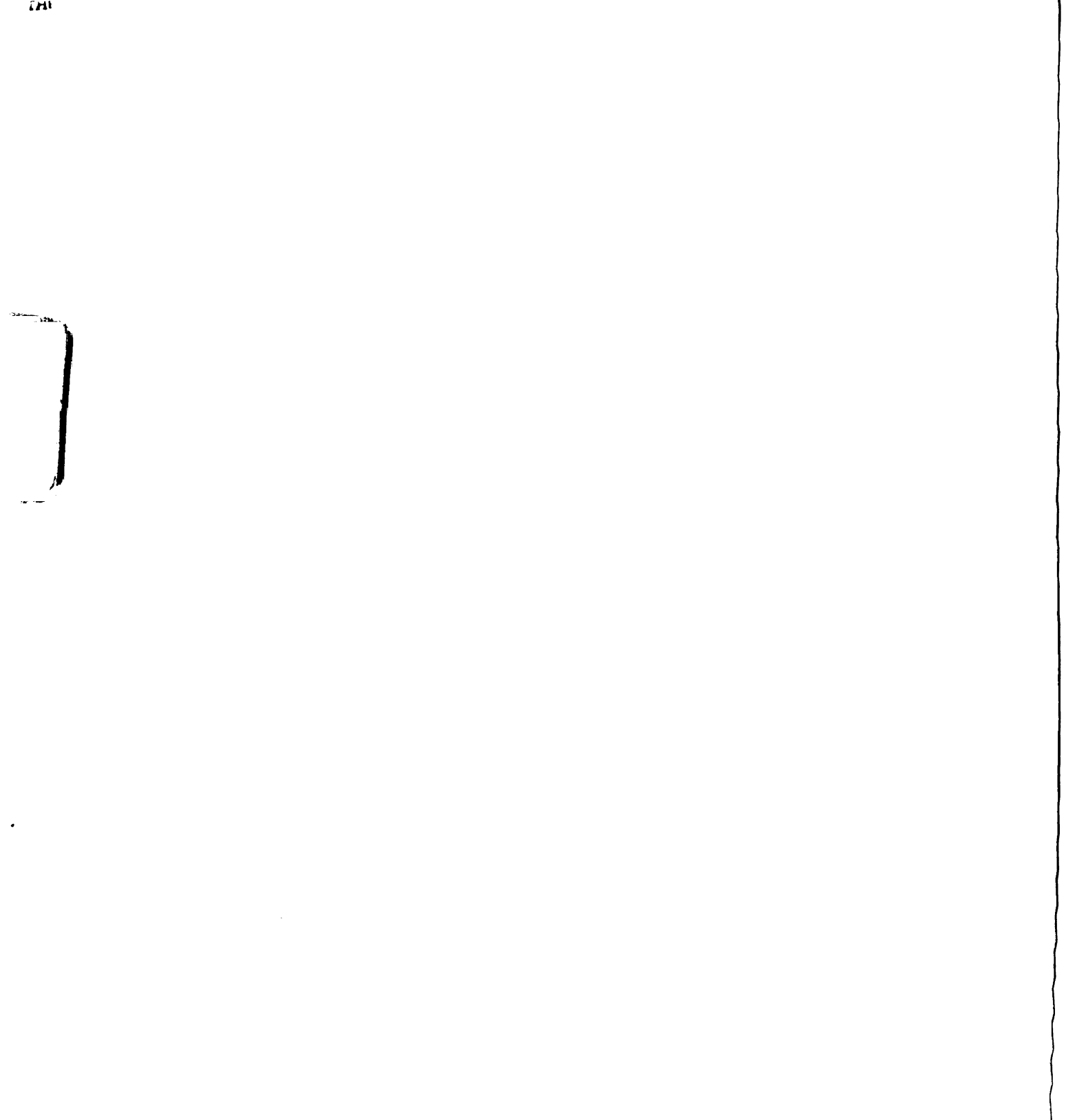
and A_2 are no longer equal, nor are the lever arms c_1 and c_2 through which the forces $\bar{\sigma}_{\mu_1}^{}A_1$ and $\bar{\sigma}_{\mu_2}^{}A_2$ act. A representative set of stress distributions is shown in the lower portion of Figure 20 for $\zeta > 90^{\circ}$, the case of interest here.

It is not difficult to accept the assumption of a shift in center of rotation when we consider the physical distances The radius of the circle of contact, as deterinvolved. mined by the compressive strength of the adherents, is approximately 0.1μ for a 10μ radius gold sphere on a plane gold substrate. Since the substrate is at the yield point (by the mere fact that a particle is resting on it), any additional compressive or shear load, such as is applied when $\zeta > 90^{\circ}$, would cause yielding. The contact area would increase since the combined stresses would meet the yield criteria. The tensile stress $\bar{\sigma}_{_{\Pi, \bullet}}$ of the resulting adhesive couple would be increased, since the area across which it is applied decreases. Thus the shift in the center of rotation resulting from increased plastic deformation for $\zeta > 90^{\circ}$ by combined applied loads, produces an increased tensile stress across portions of the interface. If this stress plus $\bar{\sigma}_{y}$ exceeds our separation (instability) criterion (i.e. $\bar{\sigma}_{\mu_1} + \bar{\sigma}_{v} > F_{n}^*/A$), then the particle must roll from its initial resting points.

To calculate $\bar{\Sigma}$, we note again that

$$F_n = F_{applied} \cos \zeta = \bar{\sigma}_v \pi b^2$$
.

The relation for the moments is modified as follows:



$$F_ta = a F_{applied} \sin \zeta = \bar{\sigma}_{\mu_1} A_1 c_1 + \bar{\sigma}_{\mu_2} A_2 c_2$$

In accordance with the ideas expressed above, and noting that $\bar{\sigma}_{\mu_1} A_1 = \bar{\sigma}_{\mu_2} A_2$, the tensile stress due to the applied couple may be written as

$$\bar{\sigma}_{\mu_1} = a F_{\text{applied}} \sin \zeta / A_1(c_1 + c_2),$$

and the compressive stress due to the applied couple as

$$\bar{c}_{\mu_2} = a F_{\text{applied}} \sin \zeta / A_2 (c_1 + c_2).$$

In view of the relative changes in A₁ and A₂ compared with the slight change in c_1+c_2 , \bar{c}_{μ_1} increases greatly and \bar{c}_{μ_2} decreases slightly as the shift, expressed as a fraction of b, increases from zero to unity.

Thus $\bar{\Sigma}$ will be increased at a given $F_{applied}$ and ζ as the axis of rotation shifts farther and farther from the center of the circle of contact. Figure 20 shows this effect quantitatively for a shift of 0.375b.

The calculations for the force of removal under these assumptions are shown in the lower curves of Figure 19.

Here are seen two sets of normalized removal forces plotted against zenith angle under the assumption that the center of rotation shifts from the center of contact to a point that is a certain fraction of the radius b from the initial center of rotation. The distance shifted is arbitrarily assumed to vary linearly with angle as ζ varies. In the first set, the shift is 0.45b, with ζ varying from 90° to 180°, 90° to 150°, and 90° to 120°. In the second set, the shift is 0.375b, with ζ varying from 90° to 120°, and 120° to 150°.

Therefore by adjusting the amount of shift of the center of rotation and the range of angle within which it shifts, we can generate normalized curves which represent very well those obtained experimentally for both gold and nickel substrates. Refinement of the assumed uniform stress distribution to a more realistic one can be done, but this would only slightly modify our adjustable parameters, namely amount of shift, angle range over which the shift takes place, and manner (rate) in which the shift takes place.

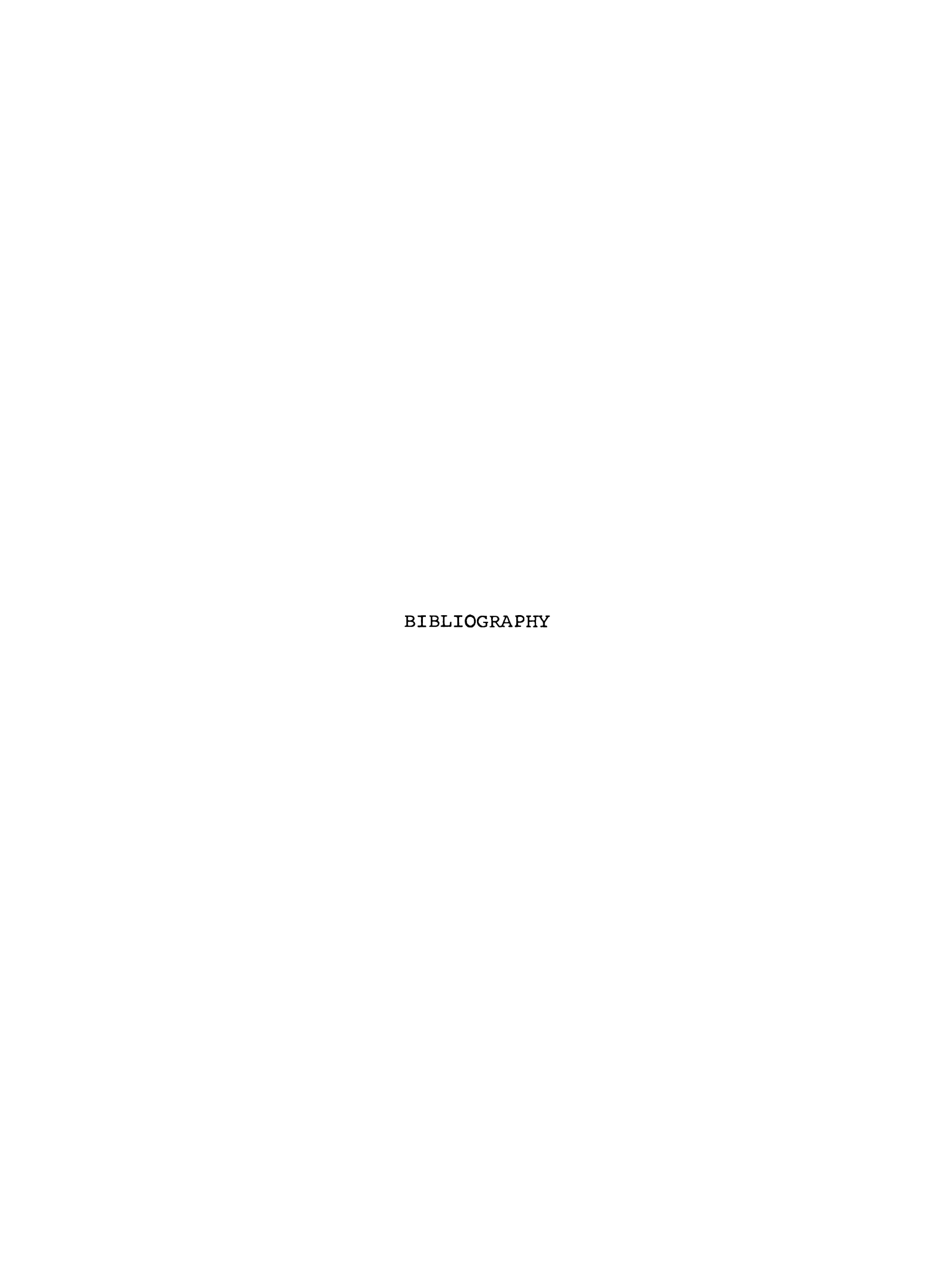
In summary, the present work demonstrates that particles are seldom removed from substrates by being pulled normally from the surface; rather they are removed by exceeding a couple resulting from the applied force. The experimental consequences of the difference in mechanism is profound, resulting in removal at certain zenith angles ζ by forces less than 1% of those required for removal at $\zeta = 0^{\circ}$. To explain this finding we assert that plastic deformation,



primarily of the substrate, is usually the controlling factor in removal. Our findings point up the necessity to look out for effects arising from unsuspected extraneous couples that may be set up by deviations from planarity, external electric fields, and so on.

To carry the investigation farther the first step would appear to be modification of the apparatus to permit continuous monitoring of the particle-substrate system. Otherwise prohibitive time is required for reaching the next level of completeness and precision. Then the model could be refined by examining, less crudely, the deformations in the materials. To test such extensions of theory, experiments with the improved apparatus could be made on materials of various mechanical properties—particularly hardness, yield strength, and tensile strength—while retaining the basic geometry of the plane and spheres of various radii. If the experiments produce confidence in the model, the concepts can be applied to different geometries, for example, discs and cubes on a plane.

Obvious extensions of the program are studies on non-metallic materials, in particular insulators, where the electric charge state introduces an important new variable. In such a program one might establish a sufficient body of principles to justify a theoretical attack on the nature of adhesive forces between solids.



BIBLIOGRAPHY

- 1. J. J. Bikerman, The Science of Adhesive Joints (New York, Academic Press, 1961), p. v.
- 2. Robert L. Patrick, "Introduction," <u>Treatise on Adhesion and Adhesives</u>, ed. Robert L. Patrick (New York, Marcel Dekker, 1967), p. 4.
- 3. P. A. M. Dirac, "Quantum Mechanics of Many Electron Systems," Proc. Roy. Soc. A-123 (1929), p. 714.
- 4. Robert J. Good, "Intermolecular and Interatomic Forces,"

 Treatise on Adhesion and Adhesives, ed. Robert L. Patrick

 (New York, Marcel Dekker, 1967), p. 64.
- 5. D. Enlow, "A Physical Study of Microbe-Surface Interactions," (General Electric Company Technical Memorandum 8126-15, October 20, 1967), p. 1.
- 6. B. R. Fish et al., Health Physics Division Annual Progress Report, July 31, 1966, ORNL-4007, pp. 245-267 passim.
- 7. Good, p. 45.
- 8. H. Krupp and G. Sperling, "Theory of Adhesion of Small Particles," J. App. Phys., 37, 11 (October 1966), p. 4180.
- 9. See e.g., R. P. Feynman et al., Lectures on Physics, cited in T. Triffet, Mechanics: Point Objects and Particles (New York, John Wiley and Sons, Inc., 1968), p. 172.
- 10. Frederick M. Fowkes, "Attractive Forces at Interfaces,"

 <u>Chemistry and Physics of Interfaces</u>, ed. David E. Gushee
 (Washington, D.C., American Chemical Society Publications, 1965), pp. 1-12.
- 11. Good, pp. 27-31.
- 12. J. J. Bikerman, "Solid-to-Solid Adhesion," Fundamental Phenomena in the Materials Sciences, Vol. 2 Surface Phenomena, ed. L. J. Bonis and H. H. Hausner (New York, Plenum Press, 1966), pp. 165-172.

- 13. J. O. Hirschfelder, C. F. Curtiss, and R. B. Bird,
 Molecular Theory of Gases and Liquids (New York, John
 Wiley and Sons, Inc., 1967), p. 25.
- 14. Hirschfelder et al., p. 26.
- 15. W. H. Keesom, Phys. Zeit., 22, 129, 643 (1921).
- 16. P. Debye, Phys. Zeit., 21, 178 (1920).
- 17. Hirschfelder et al., p. 955.
- 18. H. Margenau, "Van der Waals Forces," Revs. Mod. Phys., 11, 1 (January 1939), pp. 1-34.
- 19. F. London, "The General Theory of Molecular Forces," Trans. Farady Soc., 33, 8 (January 1937), pp. 8-26.
- 20. H. B. G. Casimir and D. Polder, "The Influence of Retardation on the London-van der Waals Forces," Phys. Rev., 73, 4 (February 15, 1948), pp. 360-372.
- 21. W. Black, J. G. V. de Jongh, J. T. G. Overbeek, and M. J. Sparnaay, <u>Trans. Farad. Soc.</u>, <u>56</u>, 1597 (1960) cited in K. W. Allen, "Strength and Structure," <u>Aspects of Adhesion 1</u>, ed. D. J. Alner (London, University of London Press Ltd., 1965), p. 15.
- 22. J. H. deBoer, <u>Trans. Farad. Soc.</u>, <u>32</u> (1936), pp. 2 ff.
- 23. H. C. Hamaker, Physica, 4, 1 (1937), pp. 1058-1071.
- 24. B. V. Deryagin and I. I. Abricossova, <u>J. Exp. Theor. Physics U.S.S.R.</u>, 30 (1956) p. 993.
- 25. J. G. Overbeek and M. J. Sparnaay, <u>Disc. Farad. Soc.</u>, <u>18</u> (1954) pp. 12 ff.
- 26. M. J. Sparnaay, Physica, 24 (1958) pp. 751 ff.
- 27. J. A. Kitchener and A. P. Prosser, <u>Proc. Roy. Soc.</u>, A 242 (1957), p. 403.
- 28. A. I. Bailey, <u>J. Appl. Phys.</u>, 32 (1961), p. 1407.
- 29. F. P. Bowden, Adhesion and Cohesion, ed. Philip Weiss (New York, Elsevier, 1962), pp. 121 ff.
- 30. F. P. Bowden and D. Tabor, The Friction and Lubrication of Solids, Part II (Oxford, Clarendon Press, 1964), passim.
- 31. K. W. Allen, <u>Aspects of Adhesion</u> 1, ed. D. J. Alner (London, University of London Press Ltd., 1965), p. 14.

- 32. G. Amontons, Memoires de l'Académie Royale, cited in F. P. Bowden and D. Tabor, The Friction and Lubrication of Solids, Part II (Oxford, Clarendon Press, 1964), p. 503.
- 33. Bowden and Tabor, pp. 242-243.
- 34. M. Corn, "Adhesion of Particles," <u>Aerosol Science</u>, ed. C. N. Davies (London, Academic Press, 1966), ch. 11.
- 35. B. B. Morgan, "The Adhesion and Cohesion of Fine Particles," <u>Brit. Coal Utiliz. Res. Assoc. Monthly Bulletin</u>, 25 (1961), cited in B. R. Fish, "The Electrostatic Forces of Adhesion Between Paricles," August 16, 1967, ORNL-TM-1947, p. 1.
- 36. N. A. Fuchs, <u>Mechanics of Aeroscls</u>, (Oxford, Pergamon Press, 1964).
- 37. J. J. Bikerman, "Solid-to-Solid Adhesion," pp. 166-169.
- 38. Bowden and Tabor, ch. 4.
- 39. Krupp and Sperling, p. 4176.
- 40. H. Krupp et al., "Haftung kleiner Teilchen an Feststoffen," Teil I, II, III, Z. angew. Phys., 16 (1964), pp. 486 ff.; 19 (1965), pp. 259 ff; 19 (1965), pp. 265 ff.
- 41. W. Kottler, H. Krupp, and H. Rabenhorst, "Adhesion of Electrically Charged Particles," Z. angew. Phys., 24 (1968) pp. 219-223.
- 42. Birney Robert Fish, "Conductive Spheres on a Charged Conductive Plane," December 1967, ORNL-4193.
- 43. B. R. Fish, "The Electrostatic Forces of Adhesion Between Particles," August 16, 1967, ORNL-TM-1947.
- 44. G. A. Tomlinson, Phil. Mag., 6 (1928), p. 695.
- 45. R. S. Bradley, Phil. Mag., 13 (1932), p. 853.
- 46. R. S. Bradley, <u>Trans. Farad. Soc.</u>, <u>32</u> (1936), p. 1088.
- 47. Daniel Eauser, "Forces of Adhesion Between Clean Metal-lic Solids," Part II, NASA N64-29219 (1964).
- 48. R. P. Abendroth and J. W. Tobias, "Use of a Recording Balance in Adhesion Studies. Application to Adhesion of Vitreous Silica to Single Crystal Gold and Silver" (Owens-Illinois, Inc. Corporate Research Report, February 26, 1969), pp. 8-10.

- 49. J. S. McFarlane and D. Tabor, <u>Proc. Roy. Soc.</u>, <u>202</u> (1950) p. 224.
- 50. P. G. Howe, D. P. Benton, and I. E. Puddington, Canadian J. Chem., 33 (1955), p. 1375.
- 51. D. Enlow, private communication.
- 52. D. W. Jordan, J. App. Phys. Suppl, 3, 5 (1954), p. S 194.
- 53. T. Gillespie, J. Colloid Sci., 10 (1955), p. 266.
- 54. L. Masironi and B. R. Fish, "Direct Observation of Particle Reentrainment from Surfaces," February 10, 1965, ORNL-1054.
- 55. R. I. Larsen, "The Adhesion and Removal of Particles Attached to Air Filter Surfaces," Am. Ind. Hyg. Assoc. J., 19 (1958), p. 265.
- 56. R. A. Bagnold, "The Re-Entrainment of Settled Dusts," Int. J. Air Poll. 2, (1960), p. 357.
- 57. F. P. Bowden and D. Tabor, The Friction and Lubrication of Solids, Part I (Oxford, Clarendon Press, 1950), p. 98.
- 58. B. Deryagin and W. Lasarew, Colloid J. Voronezh, \gtrsim (1935), p. 295.
- 59. E. Cremer, <u>Intern. Symp. Reactivity of Solids</u>, Gothenberg (1952), p. 1043.
- 60. F. Patat and W. Schmidt, Chem. Ing. Tech., 32 (1960), p. 8.
- 61. T. G. Owe Berg, M. J. Hunkins, and M. J. Stansbury, "Investigation of the Force of Adhesion Between Powder Particles" (Aerojet-General Corporation, Special Report, March 1963).
- 62. J. K. Marshall and J. A. Kitchener, <u>J. Coll. and Interface Sci.</u>, 22, (1966), pp. 342-351.
- 63. M. Hull and J. A. Kitchener, "The Study of Forces by the Rotating Disc Method," (Department of Mining and Mineral Technology, Imperial College, London).
- 64. J. W. Beams, 43rd Annual Technical Proceedings 1956, American Electroplater's Society, p. 1.
- 65. J. W. Beams, J. B. Breazeale, and W. L. Bart, <u>Phys. Rev.</u>, 100 (1955), p. 1657.

- 66. Gillespie, p. 281.
- 67. G. Bohme, H. Krupp, H. Rabenhorst and G. Sandstede, Trans. Instn. Chem. Eng. 40 (1962), p. 252.
- 68. M. Kordecki and C. Orr, Jr., "Adhesion of Solid Particles to Solid Surfaces," <u>Arch. of Envir. Health</u>, 1 (July 1960), pp. 1-9.
- 69. D. L. Enlow and P. E. Kubasko, "An Approach to the Understanding of Basic Physics Involved in Meeting Planetary Quarantine," presented at American Association for Contamination Control (May 17, 1968).
- 70. D. K. Donald, "The Electrostatic Contribution to Particle Adhesion," to be published.
- 71. Bradley, p. 853.
- 72. D. J. Montgomery, "Static Electrification of Solids,"

 Solid State Physics, Vol. 9, ed. F. Seitz and D.

 Turnbull (New York: Academic Press, 1959) pp. 144-145.
- 73. G. L. Pressman, Stanford Research Institute, Project 4375 (August 15, 1963), private communication.
- 74. Birney Robert Fish, "Conductive Spheres on a Charged Conductive Plane", p. 67.
- 75. G. L. Pressman, private communication.
- 76. J. C. Maxwell, <u>A Treatise on Electricity and Magnetism</u>, Third Edition (Oxford, Clarendon Press, 1892), Dover Reprint.
- 77. Birney Robert Fish, "Conductive Spheres on a Charged Conductive Plane", pp. 65-67.

APPENDIX



•

APPENDIX

Forces Acting on a Conductive Sphere on a Charged Conductive Plane

As part of a general program aimed at the investigation of forces of adhesion of small spheres to planar substrates by the electrostatic method, we consider the electric force tending to separate a conductive sphere from a conductive plane when an electric field is applied normal to the plane. Unfortunately, for the case of a conductive sphere on a charged conductive plane the solution is divergent and not obtainable in closed form. The difficulty arises from the inability to specify the electric-field distribution at the surface of the sphere.

Several attempts have been made to approximate the field distribution. A crude theoretical approximation to the solutions of the sphere-on-a-plane problem is the following: 75 Since the field strength on the lower half of the sphere is much less than that on the upper half, the force on the lower half is neglected. For the upper half of the sphere, a uniform radial field is assumed. Upon taking Maxwell's result for two contacting spheres for the average surface charge density, 76 applying Gauss's Law

over the upper half of the sphere for the field strength, and integrating for the total force, the following is obtained:

$$F = \pi^5 \in _0E_0^2 a^2/18 \text{ (newtons)}$$

where $\pi^5 \varepsilon_0/18 \simeq 1.505 \ x \ 10^{-10}$, a is the radius of the sphere in meters, and E_0 is the electric field strength in V/m.

An analog solution has been obtained using an electrolytic trough. The analog result for the field $E(\theta)$ at the surface of the sphere is approximated by:

 $E(\theta) = \left(0.8696 \, \cos^2 \, 1/2 \, \theta \, + \, 3.6304 \, \cos^4 \, 1/2 \, \theta \right) \, E_0 \, ,$ where E_0 is the uniform field at a large distance from the sphere. From the above field distribution, the net repulsion force can be determined by integration as

$$F_z = 1.537 \times 10^{-10} R^2 E_0^2$$
 (newtons),

where R is the radius of the sphere in meters and E_0 is the electric field strength in V/m.

To compare the above estimates with experimental values a parallel-plate capacitor was designed and built for use in conjunction with a Mettler microbalance. The bottom electrode of the capacitor is formed by a 10.16 cm x 10.16 cm x 0.32 cm polished aluminum plate. The top electrode is similar to that of the bottom, except that it has at its center a 0.025 cm-diameter hole for a conductive supporting wire. The top and bottom electrodes are spaced 5.08 cm apart. A second electrode has a 3.94 cm-diameter hole instead of a 0.025 cm-diameter hole to permit exploration of the validity

of this weighing technique by means of preliminary tests made with a circular disc and a hemisphere suspended in the hole. The Mettler balance, the top electrode, and the support wire were grounded in all experiments. Since an exact solution for the force exerted on an infinite parallel-plate capacitor or on a hemisphere resting in a parallel plate capacitor is known, a 3.78 cm-diameter circular disc was centered in the 3.94 cm-diameter hole of the top electrode of the capacitor, where it was suspended from the balance arm. A field was applied across the plate of the capacitor by applying DC potential from a Universal Voltronics, Model BAC 32 power supply. Voltage was varied from 1000 V DC to 27,000 V DC across the 5.08 cm-gap and the resulting force was measured. Care was taken to insure the planarity of the disc and the top electrode. In like fashion the relation between applied field and resulting force was determined for a 3.78 cm-diameter polished aluminized table-tennis ball. The sphere was suspended midway into the aperture, simulating the hemisphere on a plane. Figure A1 shows the relation of measured and theoretical forces for both the disc and the hemisphere.

To simulate the sphere on the plane a 0.013 cm-diameter wire was attached to a 0.87 cm-diameter sphere and passed through the 0.025 cm-diameter hole in the upper plate of the capacitor. The wire was attached to the balance arm, and the sphere was brought into contact with the upper electrode. Again, a DC voltage was incrementally increased to 27,000 V DC

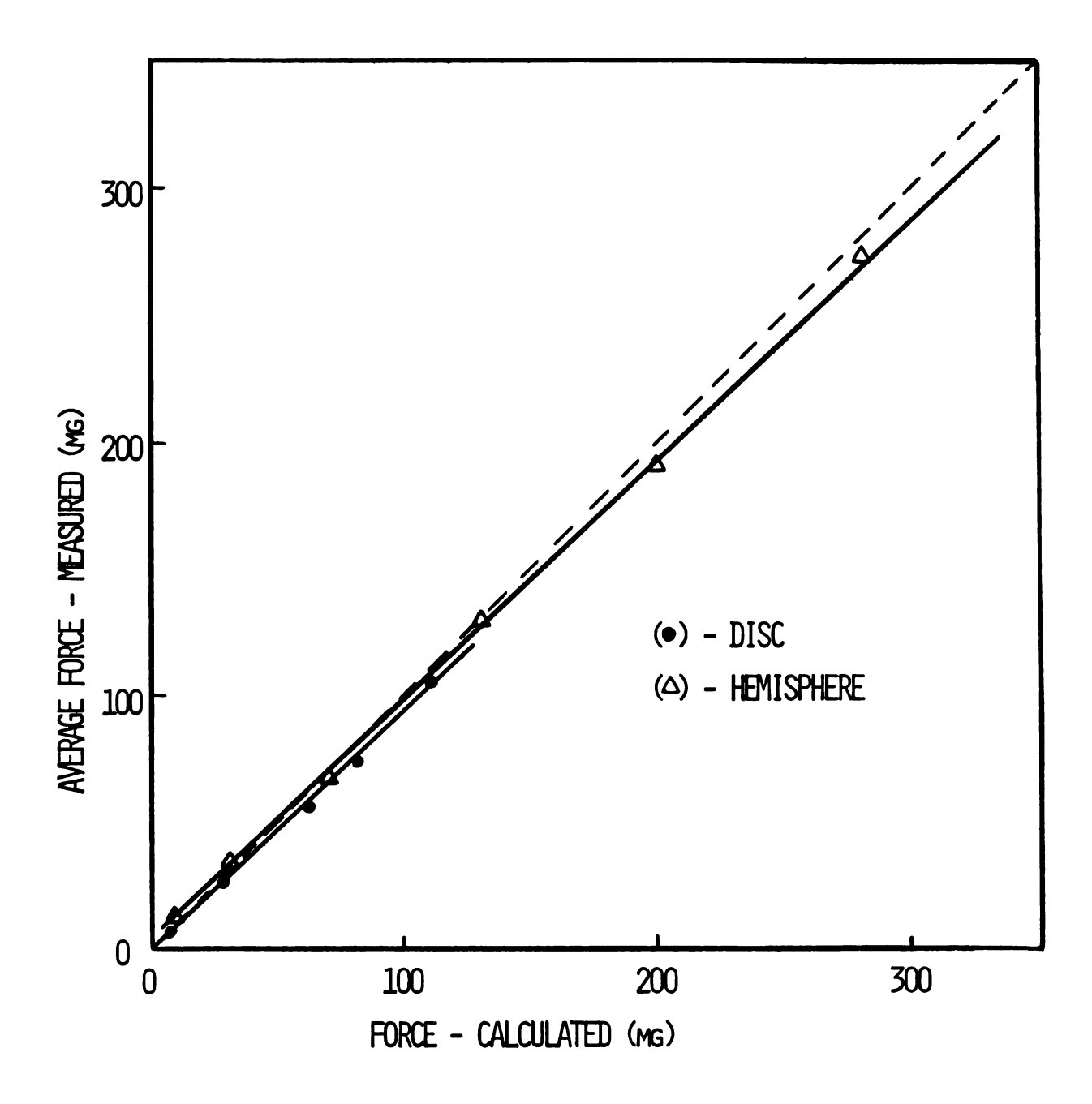


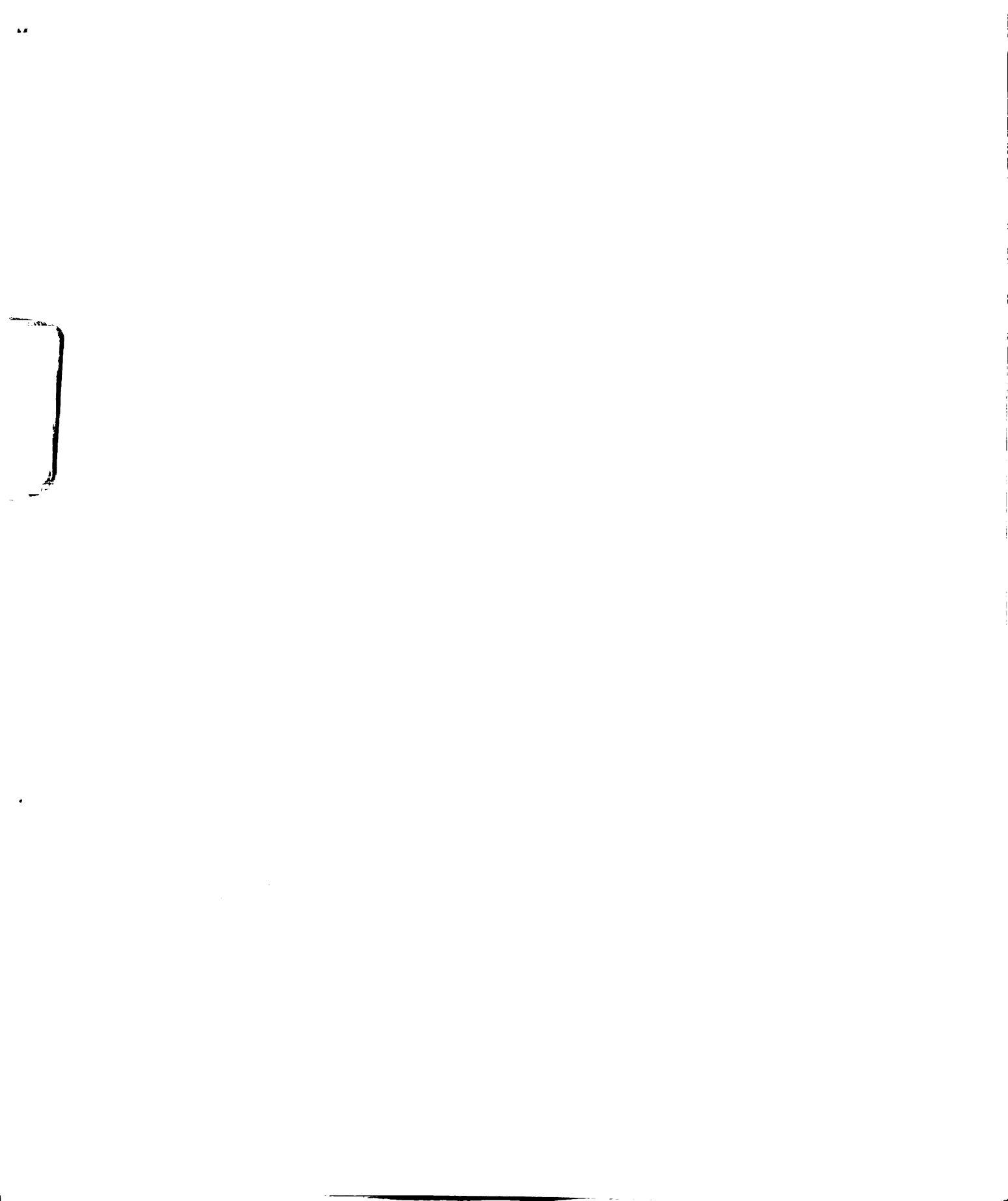
Figure A1. Measured force vs calculated force for disc and hemisphere.

and the resulting force observed. A least-squares linear fit of the measured forces against calculated forces is shown in Figure A2.

The disc and hemisphere observed force values are in good agreement with the calculated values, indicating a reasonably valid experiment. The observed forces are approximately proportional to ${\rm E_0}^2$ which suggests that the method and apparatus are appropriate for force measurements on spheres.

In the sphere-on-a-plane case, the observed force values again agree within 10% of those estimated. Since the sphere is large in proportion to the capacitor gap, it is reasonable that the observed force values are slightly larger than those predicted.

Thus it has been experimentally shown that the above formulas may be used to predict the force acting on a conductive sphere on a charged conductive plane.



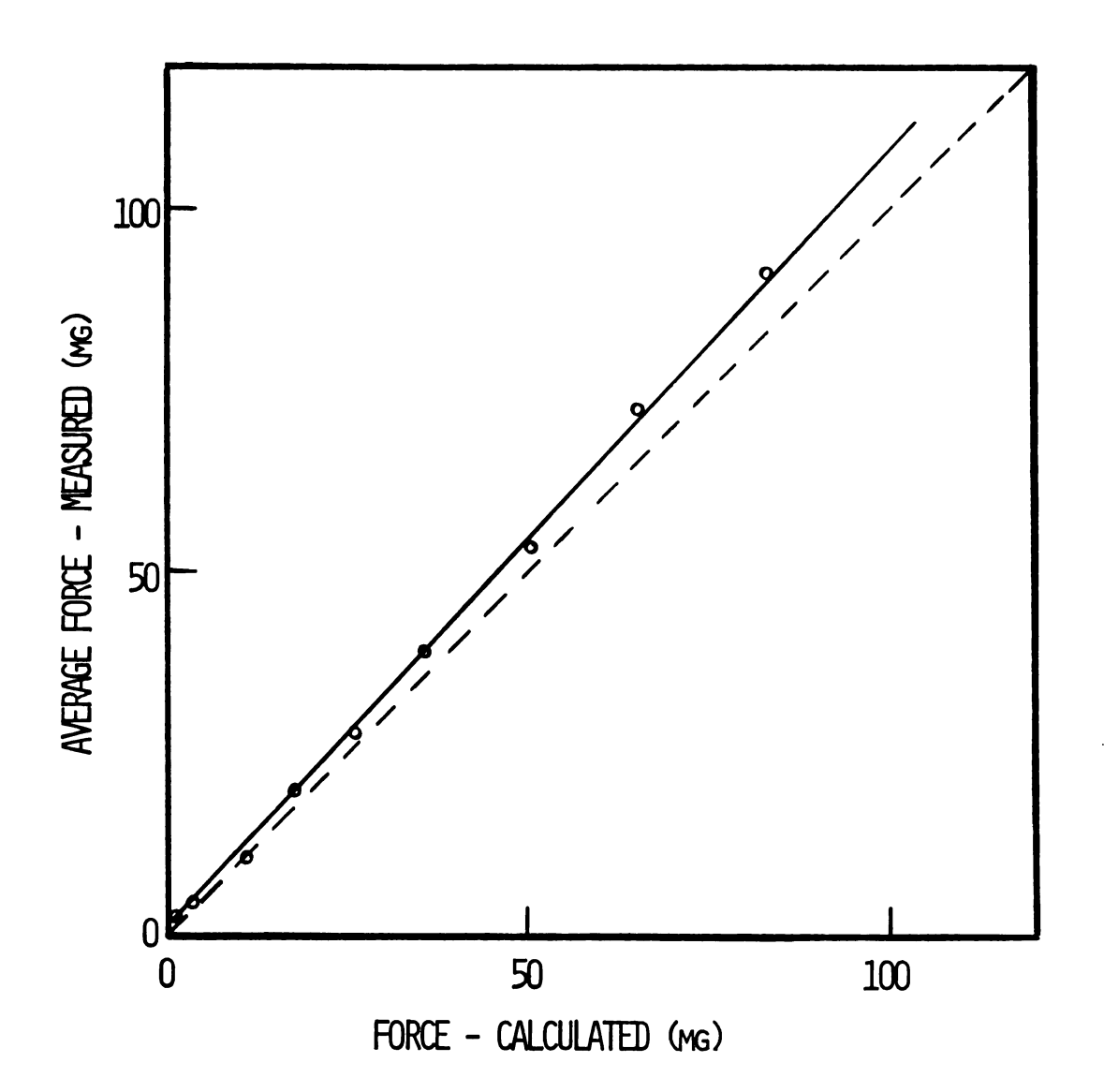


Figure A2. Measured force \underline{vs} calculated force for sphereon-a-plane.



.

ĩ h

.



